PLOS Pathogens

RESEARCH ARTICLE

T6SS4 is heterogeneously expressed in *Yersinia pseudotuberculosis* and is a target for transcriptional and post-transcriptional regulation

Anna Kerwien, Britta Körner, Ines Meyer, Yannick Teschke, Cassandra Sophie Köster, Ileana Paula Salto, Petra Dersch*, Anne-Sophie Herbrüggen*

Institute for Infectiology, Center for Molecular Biology of Inflammation (ZMBE), University of Münster, Münster, Germany

* petra.dersch@uni-muenster.de (PD); a.herbrueggen@uni-muenster.de (ASH)

OPEN ACCESS

Citation: Kerwien A, Körner B, Meyer I, Teschke Y, Köster CS, Salto IP, et al. (2025) T6SS4 is heterogeneously expressed in *Yersinia pseudotuberculosis* and is a target for transcriptional and post-transcriptional regulation. PLoS Pathog 21(9): e1013356. https://doi.org/10.1371/journal.ppat.1013356

Editor: Igor E Brodsky, University of Pennsylvania, UNITED STATES OF AMERICA

Received: July 6, 2025

Accepted: September 5, 2025

Published: September 24, 2025

Data availability statement: All relevant data are within the manuscript and its Supporting Information files and the RNA-seq data are publicly available from GEO with the identifier(s) GSE249386.

Abstract

The type VI secretion system (T6SS) is a complex secretion system encoded by many Gram-negative bacteria to translocate effector proteins directly into target cells. Due to its high complexity and energy-intensive firing process, regulation of the T6SS is tightly controlled in many organisms. *Y. pseudotuberculosis* encodes four complete T6SS clusters but lacks genes implicated in T6SS gene regulation in other microorganisms, indicating a distinct control mechanism. Here, we could show that the T6SS4 of *Y. pseudotuberculosis* is heterogeneously expressed within a population, which is determined by the transcriptional T6SS4 activator RovC. Moreover, the T6SS4 and RovC are embedded in a complex and global regulatory network, including the global post-transcriptional regulator CsrA, the *Yersinia* modulator A (YmoA), the global protease Lon, and RNases (PNP and RNase III). Post-transcriptional processing of the T6SS4 polycistron and different transcript stability within the operon also achieve a higher regulatory complexity. In summary, our work provides new insights into the sophisticated and complex regulatory network of the T6SS4 of *Y. pseudotuberculosis*, which clearly differs from regulation in other organisms.

Authors summary

Bacteria use a specialized multi-protein complex called the Type VI secretion system (T6SS) to inject toxic proteins into other cells to compete with target microorganisms or to infect host organisms. While the T6SS has been extensively studied in some model organisms, much less is known about the function and regulation of the four T6SS clusters of the food-borne human pathogen *Yersinia pseudotuberculosis*. In this study, we found that the T6SS4 of *Y. pseudotuberculosis* is only expressed in a small subpopulation *in vitro*. This suggests that

Funding: This work was supported by the University of Münster (AK, BK, IM, YT, CSK, IPS, PD, ASH) and the German Research Foundation (DFG), with grant No. DFG-STO1208/2-1 given to ASH, and grant of the priority programme SPP2002 grant No. DFG DE616/7-2 given to P. Dersch. The funders had no role in study design, data collection and analysis, decision to publish, or preparation of the manuscript.

Competing interests: The authors have declared that no competing interests exist.

its regulation is fundamentally different from what is known in other organisms. We show that a complex regulatory network regulates T6SS4 gene expression, and the T6SS4 transcript is post-transcriptionally processed, resulting in different mRNA levels of the individual T6SS components. These findings contribute to a deeper understanding of how bacteria, especially *Y. pseudotuberculosis,* regulate complex secretion systems at multiple levels.

Introduction

Bacteria in complex environmental settings are exposed to various rapidly changing conditions, such as temperature and nutrient availability, competing with other microorganisms or evading the mammalian immune system. *Yersinia pseudotuberculosis* can be found in soil, water, plants and is a human pathogen that causes various gut-associated symptoms such as diarrhea and enteritis [1–4]. Entry into the human host involves a significant temperature and nutrient composition change. Moreover, the bacteria have to switch from defending a niche against other microorganisms to evading the host's immune system, which requires a rapid and precise change in gene expression of the respective virulence factors. Due to these distinct lifestyles, it is not surprising that the expression of virulence-associated and fitness-relevant genes of *Y. pseudotuberculosis*, including its Type III (T3SS) and Type VI secretion systems (T6SS), is tightly regulated by temperature [5,6]. One well-described example is the regulation of the *Y. pseudotuberculosis* Ysc-Type III secretion system (Ysc-T3SS). The Ysc-T3SS promotes the injection of antiphagocytic Yop (*Yersinia* outer protein) effector proteins into host cells and plays an important role in defending against the attack of phagocytic cells [7–11]. Expression of the Ysc-T3SS is activated by the transcriptional regulator LcrF (low calcium-response regulator) at 37°C via an RNA-thermometer and is transcriptionally repressed at 25°C by the *Yersinia* modulator A (YmoA) [12–17]. YmoA acts as a protein thermometer as it undergoes a conformational change and is rapidly degraded by the Lon/ClpP proteases upon a temperature upshift from moderate (25°C) to body temperature (37°C) [14,16].

In contrast to the regulation of the T3SS, much less is known about the regulation of the four T6SS clusters of *Y. pseudotuberculosis,* differing in their chromosomal arrangement and number of genes [18]. Exclusively encoded in Gram-negative bacteria, T6SSs are large contact-dependent secretion systems of 13 highly conserved core components that directly translocate a broad spectrum of different effector proteins into competing prokaryotic or eukaryotic cells [19–25]. As the assembly and disassembly of the apparatus are very energy-consuming, we expected that the expression of T6SSs of *Y. pseudotuberculosis* would be tightly regulated in response to environmental signals, as observed in other microorganisms [26–29]. Previous studies on the T6SS4 gene cluster of *Y. pseudotuberculosis* revealed that its expression is strongly temperature-dependent. It can only be induced at moderate growth temperature (25°C), predominantly during the stationary phase, but not at 37°C *in vitro* [18,30]. It was also found that expression of T6SS4 is promoted by direct

binding of global regulators such as RpoS, OmpR, or RovM, and T6SS4 expression is positively regulated by quorum sensing [18,31–34]. Unlike any other yet known T6SS, *Yersinia*-T6SS4 gene expression further requires the expression of the specific hexameric transcriptional activator RovC [30]. RovC is encoded in the opposite direction upstream of the T6SS4 cluster and activates T6SS4 gene expression by direct binding within the T6SS4 promoter region [30]. The T6SS4 of *Y. pseudotuberculosis* is additionally controlled by the global regulator CsrA (carbon storage regulator A) [30]. The CsrA protein belongs to the Csr system, which includes two small non-coding RNAs CsrB and CsrC. They can bind and sequester multiple CsrA proteins, thus preventing CsrA from binding to its target mRNAs. The Csr system is known to be an important post-transcriptional regulatory system that influences the expression of many virulence- and fitness-relevant genes in bacteria [35–38]. In *Y. pseudotuberculosis*, CsrA was found to play an essential role in T6SS4 expression, as it affects *rovC* on the transcriptional and post-transcriptional levels [30]. Although the exact mechanism of how CsrA influences RovC synthesis is still unclear, CsrA was shown to repress the *rovC* transcription indirectly, but also to stabilize *rovC* mRNA, indicating a complex role in the regulation of RovC and, thus, of T6SS4 [30]. It is further known that the CsrA homologous protein RsmA (regulator of secondary metabolites A) negatively regulates the expression of all three T6SS islands in *Pseudomonas aeruginosa*, highlights the critical role of the Rsm/Csr system in T6SS regulation [39].

As several studies have shown that the expression of the T6SS4 is repressed at 37°C [18,30,31], it can be assumed that T6SS4 targets (micro-)organisms other than mammals, *e.g.*, competing bacteria in their environmental niches. However, no antibacterial effector that is exclusively translocated by T6SS4 has yet been identified. In contrast, it was hypothesized that *Y. pseudotuberculosis* uses its T6SS4 to maintain the intracellular ion homeostasis of, *e.g.*, manganese or zinc [40–43]. This suggests a role in the resistance to oxidative stress and could promote a higher virulence in mice [40,42,43]. However, no expression of the T6SS4 was detectable by RNA-sequencing under different virulence-relevant conditions at 37°C and during infection in other studies [6,44–47].

To gain further insight into the role of the T6SS4, its temperature control mechanisms, and function, we analyzed the expression control of the *Y. pseudotuberculosis* T6SS4 at transcriptional, post-transcriptional, and translational levels. To this end, we used a flow cytometry-based approach to study T6SS4 expression at a single-cell level. We found that T6SS4 cluster expression within a population is very heterogeneous, unlike T6SS gene clusters in *Vibrio* or *Pseudomonas* spp [19,22,23,26,48–50]. We could further show that the heterogeneous expression of the transcriptional regulator gene *rovC* promotes phenotypic heterogeneity. Moreover, heterogeneous *rovC* and T6SS4 gene expression are impacted by the global protease Lon, the RNases PNPase and RNase III, the RNA-binding protein CsrA, and the transcriptional regulator YmoA. The rapid downregulation of *rovC* and T6SS4 gene expression upon temperature shift from 25°C to 37°C involves distinct temperature-dependent post-transcriptional modifications of both *rovC* and T6SS4 mRNA.

Results

Flow cytometry-based method revealed heterogeneous expression of the T6SS4 at different temperatures

In previous studies, T6SS4 expression of *Y. pseudotuberculosis* was mainly studied in bulk approaches, revealing only an overall up- or downregulation of gene expression in a bacterial population [18,31,34]. In contrast to this general approach to analyze gene expression, we applied flow cytometry and fluorescence microscopy to study T6SS4 expression at a single-cell level. Therefore, we used a strain in which the core gene *clpV4* of the T6SS gene cluster 4 (T6SS4) is chromosomally fused to *gfp* (Fig 1A). We could show that only a small subpopulation (approximately 10–15%) highly expressed *clpV4-gfp* (T6SS4-ON subpopulation), whereas the majority of the population remained repressed (T6SS4-OFF subpopulation) (Figs 1B and S1). This finding of phenotypic heterogeneity—referring to variable T6SS4 expression within a genetically identical population—differs from what was found in *P. aeruginosa* and *Vibrio cholerae*. In these model organisms, T6SS gene cluster expression was reported to be homogeneous among genetically identical cells [22,48,51–53]. To analyze a higher bacterial cell number, a flow cytometry-based method was established by gating for GFP-positive (GFP^+, T6SS4-ON) and negative (GFP^-, T6SS4-OFF) subpopulations (Figs 1C and S2). Incubation at 25°C resulted in an

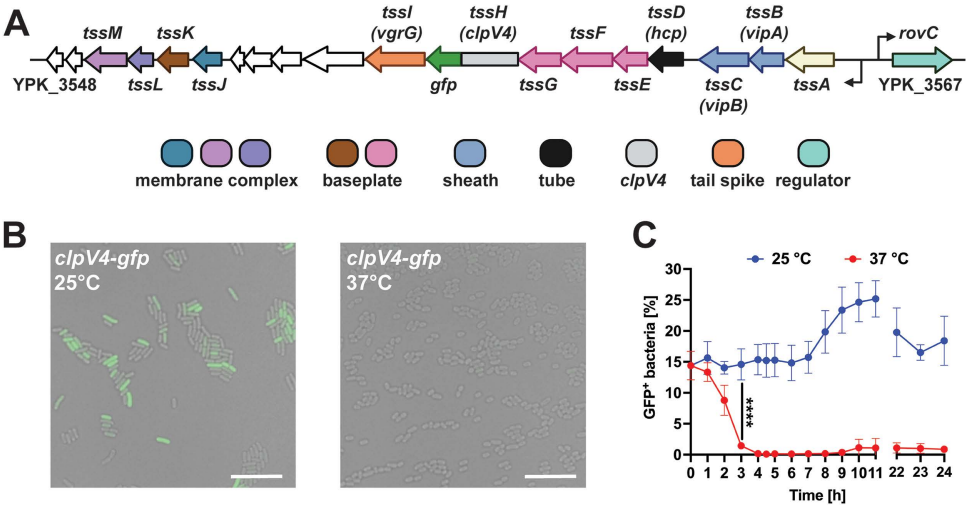

Fig 1. T6SS4 of *Y. pseudotuberculosis* YPIII is heterogeneously expressed. (A) Scheme of YPIII T6SS4 cluster. Chromosomal fusion of *clpV4* to *gfp* was used as a reporter to analyze expression of T6SS4 genes. **(B)** Fluorescence microscopy of wt *clpV4-gfp*. The bacteria were incubated for 6 h at 25°C or 37°C and imaged on 1% agarose pads. The scale bar represents 10 μm, and representative overlays of the GFP channel and brightfield are shown. **(C)** Quantification of *clpV4-gfp* expressing bacteria (GFP^+) incubated at 25°C or 37°C. 1 x 10^5 bacteria were analyzed using flow cytometry. Data depict the mean and standard deviation of three independent experiments. Statistical differences were determined using a Two-Way ANOVA with Šidák correction. **** = $p \leq 0.0001$.

https://doi.org/10.1371/journal.ppat.1013356.g001

increasing amount of *clpV4-gfp* expressing bacteria after 8 h, when the cultures reached the stationary phase. In contrast, *clpV4-gfp* expression was rapidly downregulated after a temperature shift to 37°C and remained repressed throughout the bacterial growth phase (Fig 1B and 1C). This aligns with previous findings, describing a strong regulatory effect of temperature and growth phase on the T6SS4 expression [18]. It also illustrates that the overall induction of the T6SS4 expression is only triggered in a subset of the population.

The heterogeneous expression of the transcriptional regulator gene *rovC* causes heterogeneity of T6SS4

Our previous study revealed that expression of T6SS4 genes is activated by the hexameric transcriptional regulator RovC. It was further shown that deletion of *rovC* completely abolishes T6SS4 expression at 25°C [30]. Therefore, we assumed that *rovC* might only be expressed in the T6SS4-ON subpopulation. To test this hypothesis, we introduced a low-copy-number plasmid containing the translationally fused promoter region of *rovC* to *mCherry* (S2 Fig) into the *Y. pseudotuberculosis* strains expressing the chromosomally encoded *clpV4-gfp* fusion. With this dual reporter strain, the expression of *rovC-mCherry* and *clpV4-gfp* was analyzed simultaneously. As shown in Fig 2A, the *rovC-mCherry* fusion was weakly expressed in the majority of the bacteria ($mCherry^{low}$ population), and these bacteria did not express *clpV4-gfp* (Fig 2B and 2C). In contrast, 15–20% of the bacteria showed a high expression level of *rovC-mCherry* and expressed *clpV4-gfp*. This strongly indicates that the heterogeneous expression of the transcriptional regulator gene *rovC* causes heterogeneity of T6SS4 expression.

Influence of the global post-translational, post-transcriptional, and transcriptional regulators Lon, CsrA, and YmoA on temperature-dependent *rovC* and T6SS4 gene expression

Next, we aimed to gain insight into the molecular mechanisms of how heterogenous T6SS4 expression is controlled in response to temperature, *e.g.*, which factors contribute to the rapid decrease of the number of T6SS4-ON bacteria in the population upon a temperature shift from 25°C to 37°C. Several global regulators of *Yersinia* have been shown to control

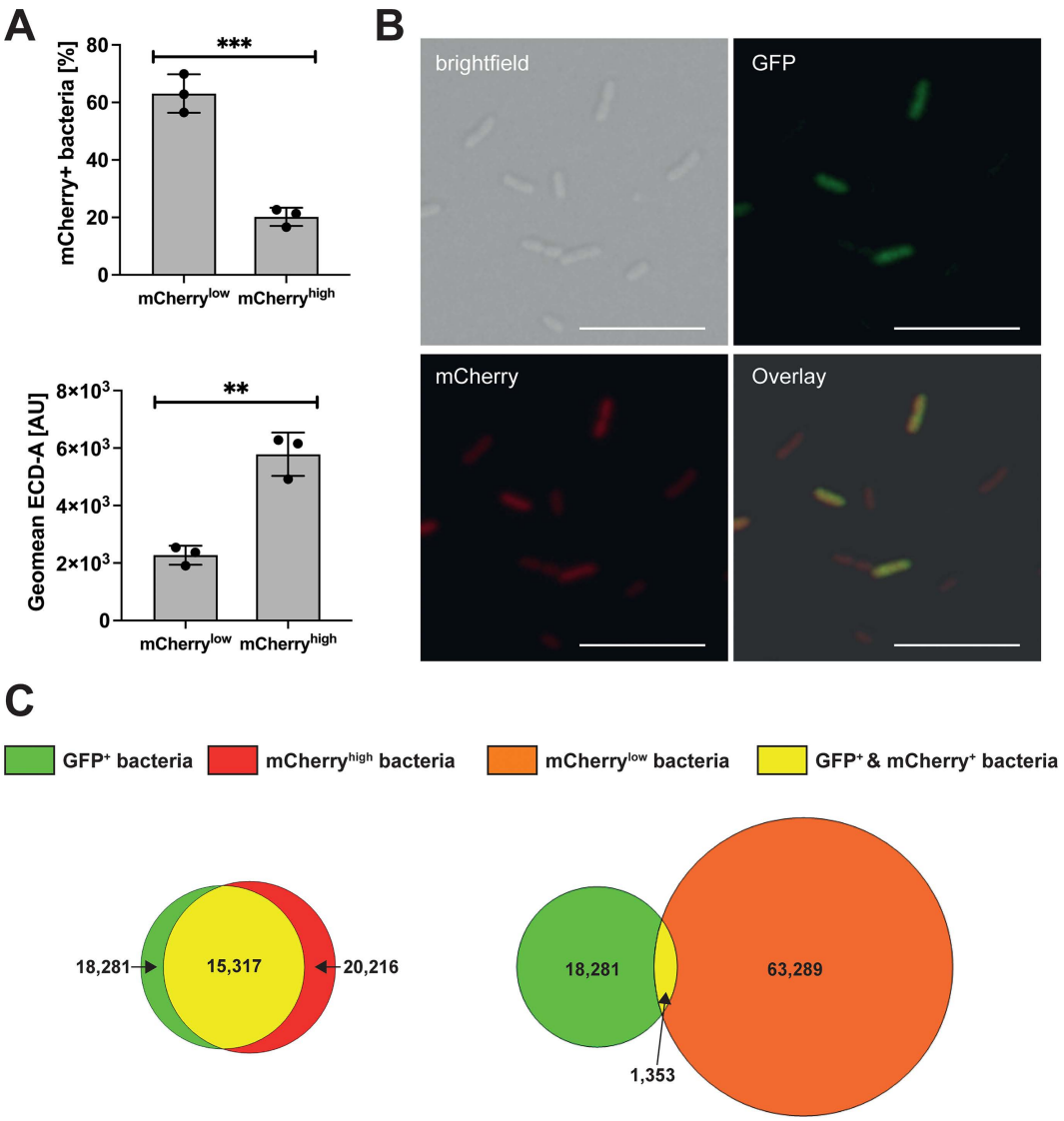

Fig 2. Heterogeneous T6SS4 expression is determined by RovC. (A) Flow cytometric analysis of a translational *rovC* promoter fusion to mCherry (pP_{rovC} *rovC'-'mCherry*) resulted in two subpopulations of mCherry^{low} and mCherry^{high} expression, which differed in their expression intensity (GeoMean ECD-A). Significant differences were determined using an unpaired t-test. **(B)** Fluorescence microscopy of *Y. pseudotuberculosis* YPIII *clpV4-gfp* pP_{rovC} *rovC'-'mCherry*. Images of brightfield, GFP, and mCherry channel are shown, as well as an overlay of all channels. Representative images from one of three independent experiments are shown. Scale bar indicates 10 μm. **(C)** Quantitative Venn diagram of *mCherry* and *gfp* expressing bacteria, analysed by flow cytometry of wt *clpV4-gfp* with translational fusion of promoter region of *rovC* to *mCherry* (pP_{rovC} *rovC'-'mCherry*). 1 x 10^5 bacteria were analysed. Data depict the mean of three independent experiments. Absolute numbers of GFP-expressing bacteria (green), mCherry^{high}-expressing bacteria (red), mCherry^{low}-expressing bacteria (orange), and bacteria expressing both (yellow). ** = p ≤ 0.01, *** = p ≤ 0.001.

https://doi.org/10.1371/journal.ppat.1013356.g002

gene expression in a temperature-dependent manner. One example is the global protease Lon [54–59], which was shown to be involved in the temperature-dependent degradation of the virulence regulators YmoA and RovA of *Y. pestis* and *Y. pseudotuberculosis,* respectively [60,61]. We first examined whether the Lon protease affects the number of T6SS4-ON bacteria in a temperature-dependent manner. We found that deleting the *lon* gene substantially increased *clpV4-gfp* (T6SS4-ON)-expressing bacteria at 25°C compared to the wildtype (Fig 3A). However, the number of the *clpV4-gfp*

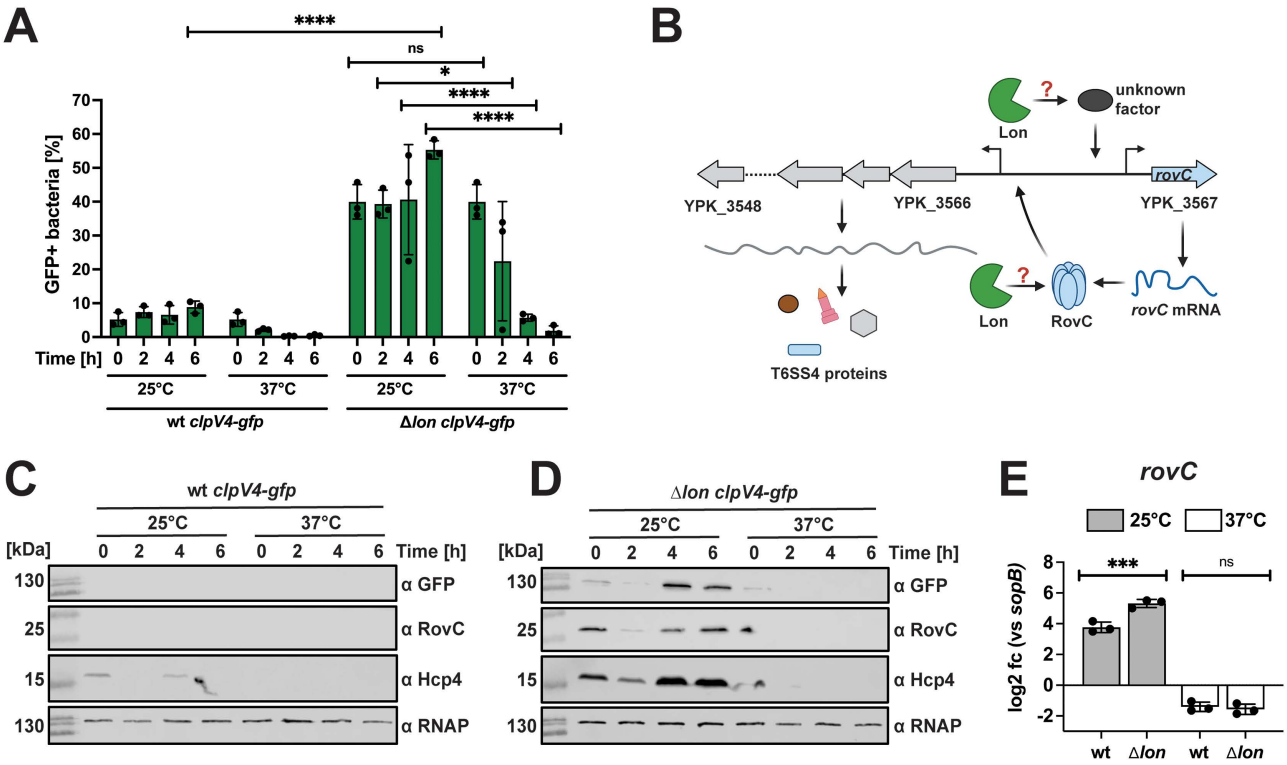

Fig 3. Temperature-based downregulation is not due to Lon-mediated degradation at 37°C. (A) Quantification of *clpV4-gfp* expressing bacteria in wt *clpV4-gfp* (YP412) and Δ*lon clpV4-gfp* (YP544) at either 25°C or 37°C. 1 x 10^5 bacteria were analyzed using flow cytometry. Data depict the mean and standard deviation of three independent experiments. Significant differences were determined using a Two-Way ANOVA with Šidák correction. **(B)** Scheme of potential downregulation at 37°C mediated by Lon-dependent inhibition of the *rovC* transcription or by Lon-mediated proteolysis of RovC. Created in BioRender. Dersch, **P.** (2025) https://BioRender.com/8el9map. **(C-D)** Western blotting of wt *clpV4-gfp* and Δ*lon clpV4-gfp*. Protein levels of ClpV4-GFP, RovC, and Hcp4 were detected using antibodies against GFP, RovC, and Hcp4. Detection of RNAP was used as a loading control. Experiments were performed in three independent replicates; one representative Western blot is shown. (E) qRT-PCR was performed of total RNA extracted from wt and Δ*lon* incubated for 6 h at 25°C or 37°C. Specific primer pairs were used to determine expression levels of *rovC,* and log2 fold changes to *sopB* as a non-temperature-regulated reference gene [6] were calculated. Experiments were performed in three independent replicates, and the mean and standard deviations are shown. Significant differences were determined using an unpaired t-test. * = p ≤ 0.05, *** = p ≤ 0.001, **** = p ≤ 0.0001, ns = not significant p > 0.05.

https://doi.org/10.1371/journal.ppat.1013356.g003

(T6SS4-ON)-expressing bacteria decreased rapidly when the culture was shifted from 25°C to 37°C. Based on this result, it is possible that Lon directly targets RovC or influences *rovC* transcription indirectly (Fig 3B). Western blot analysis demonstrated that the levels of T6SS4 components, such as Hcp4 and ClpV4, as well as the T6SS4 activator RovC are strongly increased in the absence of Lon at 25°C but not at 37°C (Fig 3C and 3D). This indicates that Lon exerts its influence on T6SS4 gene expression via the regulation of RovC. We further tested the impact of the *lon* gene deletion on the number of *mCherry*^{high} (RovC-ON) bacteria in *Y. pseudotuberculosis* expressing the P_{rovC}*rovC'-'mCherry* reporter (S3 Fig) and the overall amount of the *rovC* transcript in the bacterial cells (Fig 3E). We found a higher number of RovC-ON bacteria and a significant increase in *rovC* transcript levels in the *lon* deletion mutant at 25°C. In contrast, the *rovC* transcript was downregulated at 37°C independently of the presence of Lon (Fig 3E), indicating that Lon controls the overall level of RovC but is not involved in temperature control.

Previous work has shown that the expression of the Csr system components of *Yersinia,* which are known to repress RovC and thus T6SS4 synthesis [30], is strongly controlled by temperature and carbon/nutrient sources [16]. CsrA regulates RovC synthesis in opposing ways: it represses transcription while promoting post-transcriptional

stability [30]. Moreover, a *Yersinia*-specific histone-like protein YmoA, with homology to the *E. coli* Hha protein, is known to regulate *Yersinia* virulence factors, including the master regulator LcrF of the Ysc-T3SS gene cluster in a temperature-dependent manner [12,13]. From a transcriptomic analysis, it is further known that YmoA also influences the expression of several virulence-associated genes, such as *vipA4*, *vipB4,* and *rovC* in *Y. pseudotuberculosis*, and modulates the expression of the Csr system [12,15,16]. Based on this knowledge, we used *csrA* and *ymoA* deletion strains to test their influence on the synthesis of RovC and T6SS4 components at 25°C and 37°C (Fig 4A). A deletion of *csrA* or *ymoA* resulted in a significant increase in the number of T6SS4-ON bacteria at 25°C (Fig 4B), whereby the overall expression was significantly higher in the Δ*csrA* compared to the Δ*ymoA* mutant strain (Fig 4B and 4C). In addition, both gene deletions also led to a substantial increase in the RovC and Hcp4 levels at 25°C compared to wt (Fig 4D). However, no upregulation of RovC and the T6SS4 components was observed in the mutant strains at 37°C (Fig 4B-D). A qRT-PCR analysis further showed that *rovC* and T6SS4 gene transcript levels decreased significantly between 25°C and 37°C in both mutants (Figs 4E and S4), indicating that CsrA and YmoA affect RovC and T6SS4 expression but are not involved in temperature control.

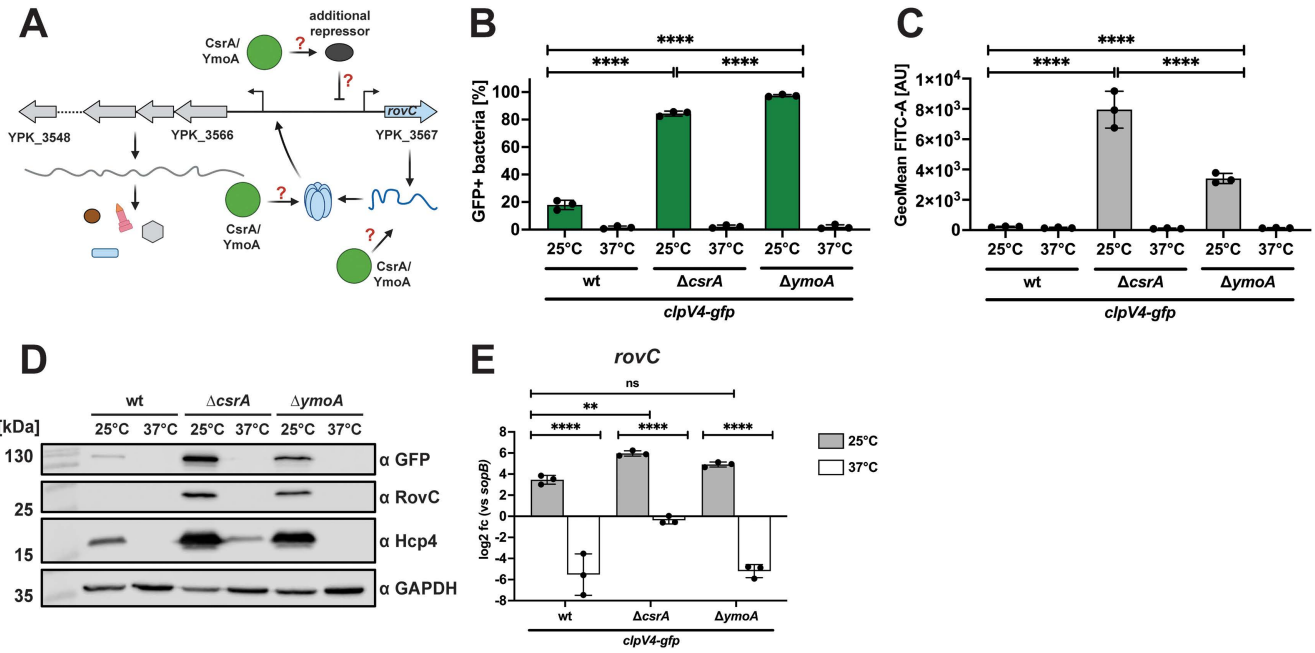

Fig 4. Influence of CsrA and YmoA on the temperature-controlled RovC and T6SS4 components synthesis. (A) Schematic overview of potential regulation pathways, controlling the temperature-dependent synthesis of RovC and T6SS4. Regulation can be mediated by an independent repressor or by affecting transcript or protein stability on a post-transcriptional level. Created in BioRender. Dersch, **P.** (2025) https://BioRender.com/9cztzkr. **(B-C)** Quantification of *clpV4-gfp* expressing bacteria (B) and GFP expression intensity (GeoMean FITC-A) (C) using the wt *clpV4-gfp* (YP412), Δ*csrA clpV4-gfp* (YP559), and Δ*ymoA clpV4-gfp* (YP474) strains incubated overnight at either 25°C or 37°C. 1 x 10^5 bacteria were analyzed using flow cytometry. Data depict the mean and standard deviation of three independent experiments. Significant differences in B) and C) were determined using a Two-Way ANOVA with Tukey's correction. **(D)** Western blotting of samples analyzed in **(B)**. ClpV4-GFP, RovC, and Hcp4 protein levels were detected using antibodies against GFP, RovC, and Hcp4. RNAP was detected as a loading control. Experiments were performed in three independent replicates; one representative Western blot is shown. **(E)** Total RNA of an overnight culture of wt, Δ*csrA* (YP53), and Δ*ymoA* (YP50) was isolated to perform qRT-PCR. Specific primer pairs for *rovC* were used to determine the expression of *rovC*. Log2 fold changes were calculated between *rovC* and *sopB* as a non-temperature-regulated reference gene [6]. Experiments were performed in three biological replicates, and significant differences were determined using a Two-Way ANOVA with uncorrected Fisher's LSD. ** = p ≤ 0.01, **** = p ≤ 0.0001, ns = not significant, p > 0.05.

https://doi.org/10.1371/journal.ppat.1013356.g004

Downregulation of T6SS4 expression at 37°C is promoted by post-transcriptional control of *rovC* mRNA levels

A previous experiment in this study comparing *rovC* mRNA levels at different temperatures revealed that the amount of *rovC* transcripts is significantly reduced at a growth temperature of 37°C compared to 25°C (Figs 3E and 4E). To gain further insight into the mechanism underlying temperature control, we tested the expression of the *rovC* gene in response to temperature using a translational reporter fusion (pP_{rovC}*rovC'-'mCherry*). As shown in Fig 5A, no major shifts of the *rovC-mCherry*^{high} and *rovC-mCherry*^{low} populations were detectable after 6 h of incubation at 37°C. Although similar numbers of *rovC-mCherry*^{high} expressing bacteria were detectable 6 h after the temperature upshift, we could only detect *clpV4-gfp* (T6SS4-ON) expressing bacteria in cultures grown at 25°C (Figs 5A, 5B and S5), indicating that the activity of the *rovC* promoter is not subjected to temperature control.

Based on the fact that the amount of *rovC* transcript was significantly reduced at 37°C compared to 25°C, as demonstrated by qRT-PCR (Figs 3E and 4E), and by an RNA-sequencing analysis [6], we hypothesized that the *rovC* mRNA is a potential target of temperature-controlled RNase-mediated degradation. To test this, we analyzed *rovC* transcript levels in mutant strains lacking different RNase genes identified in *Y. pseudotuberculosis* YPIII [46]. We found that *rovC* transcript levels in bacteria grown at 25°C were significantly increased in mutants in which the polynucleotide phosphorylase (Δ*pnp*) or the RNase III gene (Δ*rnc*) was deleted (Fig 5C). The increase in *rovC* transcript levels was considerably more pronounced in the Δ*pnp* mutant compared to the Δ*rnc* mutant. We also performed a comparative *rovC* transcription profile analysis of the wildtype and both RNase mutants using an RNA-sequencing data set from our previous study [46]. As shown in Fig 5D and 5E, the overall read pattern covering the *rovC* gene is comparable, and no typical changes of the sequencing read patterns due to the processing by RNases were detectable [62–64]. This suggests that the influence of the RNases on *rovC* transcript levels is not direct. Furthermore, we revealed that the *rovC* mRNA amount was still significantly reduced at 37°C in both mutants compared to 25°C (Fig 5C). Hence, both RNases control the synthesis of RovC but do not seem to be mainly involved in their temperature control.

To further investigate *rovC* transcript stability, we artificially overexpressed *rovC* encoded on a medium copy plasmid from a temperature-insensitive, arabinose-inducible promoter to exclude regulatory mechanisms influencing *rovC* transcription (Fig 6A). We found that RovC-overexpression under the control of the P_{BAD} promoter resulted in the synthesis of RovC at 37°C (Fig 6B). However, the overall amount of detectable RovC was 1.38 x higher when *rovC* was overexpressed at 25°C (Fig 6C). Accordingly, *rovC* transcript levels were higher at 25°C after induction (Fig 6D), emphasizing a post-transcriptional regulation of *rovC* mRNA levels in response to temperature. We further tested how overexpression of *rovC* under these conditions influences the induction of the T6SS4 gene cluster. For this purpose, we used a P_{T6SS4}*tssA4'-'gfp* reporter fusion in which the predicted T6SS4 promoter [18] and the first codons of the first gene of the operon (*tssA4*, Fig 1A) are fused to *gfp*. As shown in Fig 6E and 6F, three hours after induction of *rovC* overexpression both, the number of GFP-expressing bacteria and the overall expression of the *gfp* reporter fusion were significantly increased at 25°C and 37°C compared to empty vector controls. In line with *rovC* transcript and RovC protein levels in the bacteria (Fig 5B and 5D), the number of T6SS-ON bacteria and the overall expression of the P_{T6SS4}*tssA'-'gfp* reporter fusion was still higher at 25°C compared to 37°C. This further indicates that RovC is fully functional at 37°C when overexpressed from an alternative promoter, and thermally induced changes in the protein folding and/or quaternary structure of RovC triggered by the temperature upshift do not seem to be important for T6SS4 expression control.

Processing of the T6SS4 polycistronic mRNA leads to differential expression of T6SS4 genes in response to temperature

In our attempt to analyze how RovC influences T6SS4 transcript levels at different temperatures, we also tested the expression of the translational *clpV4-gfp* fusion after *rovC* overexpression (Fig 7A). Even though the P_{T6SS4} promoter was highly induced at 37°C in approximately 70% of the bacteria (Fig 6E), we could not detect an equivalent induction with the *clpV4-gfp* fusion. Compared to 25°C with 90% GFP-positive bacteria (T6SS4-ON), less than 5% of the population could

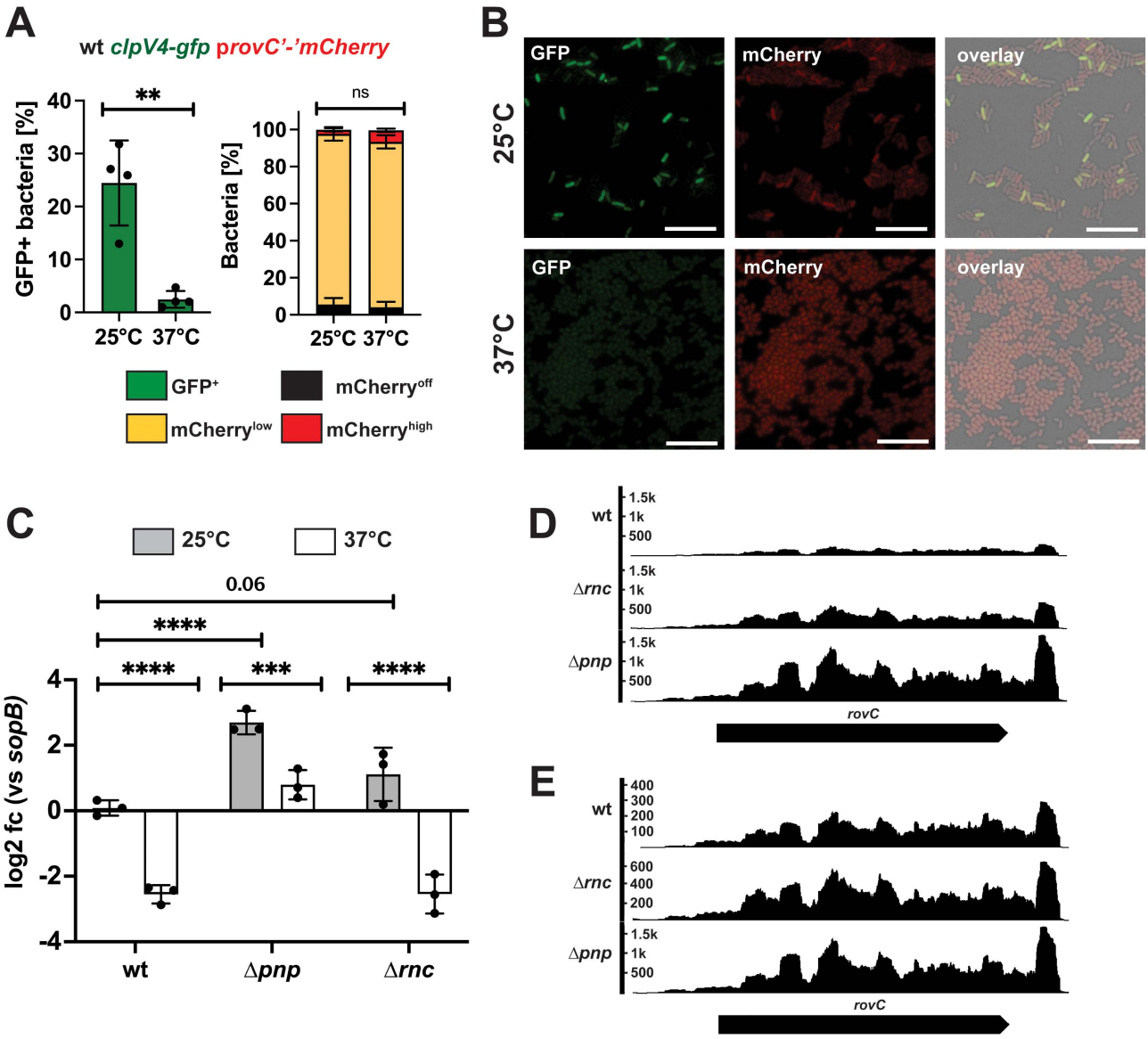

Fig 5. *rovC* mRNA transcript is post-transcriptionally modified at 37°C. (A) Wt *clpV4-gfp* expressing a plasmid-encoded P_{rovC} *rovC'-'mCherry* fusion was incubated for 6 h at 25°C or 37°C, and *gfp*- and *mCherry*-expressing bacteria were quantified by flow cytometry. 1 x 10^5 bacteria were analyzed for each time point using flow cytometry. Experiments were performed in four independent replicates; the mean and standard deviation are shown. Significant differences of GFP⁺ bacteria at 25°C and 37°C were determined using an unpaired t-test and of *mCherry*-expressing bacteria using a Two-Way ANOVA with Tukey's correction. **(B)** Fluorescence microscopy of wt *clpV4-gfp provC'-'mCherry* after 6 h of incubation at 25°C or 37°C. Representative images of the GFP and mCherry channels and an overlay of the brightfield and the GFP and mCherry channels were shown. Bacteria were imaged on agarose pads containing 1% agarose, and the scale bar represents 10 μm. **(C)** qRT-PCR was performed with total RNA extracted from wt, Δ*pnp*, and Δ*rnc* incubated for 2 h at 25°C or 37°C. Specific primer pairs were used to determine expression levels of the *rovC* gene, and log2 fold changes to *sopB* as a non-temperature-regulated reference gene [6] were calculated. Experiments were performed in three independent replicates, and significant differences were determined using a Two-Way ANOVA with Tukey's correction. **(D-E)** RNA coverage of the *rovC* gene of wt, Δ*pnp*, and Δ*rnc*, incubated for 2 h at 25°C with the same scale **(D)** and an adjusted scale **(E)**. Data were taken from Meyer *et al*. [46]. * = p ≤ 0.05, ** = p ≤ 0.01, *** = p ≤ 0.001, **** = p ≤ 0.0001, ns = not significant p > 0.05.

https://doi.org/10.1371/journal.ppat.1013356.g005

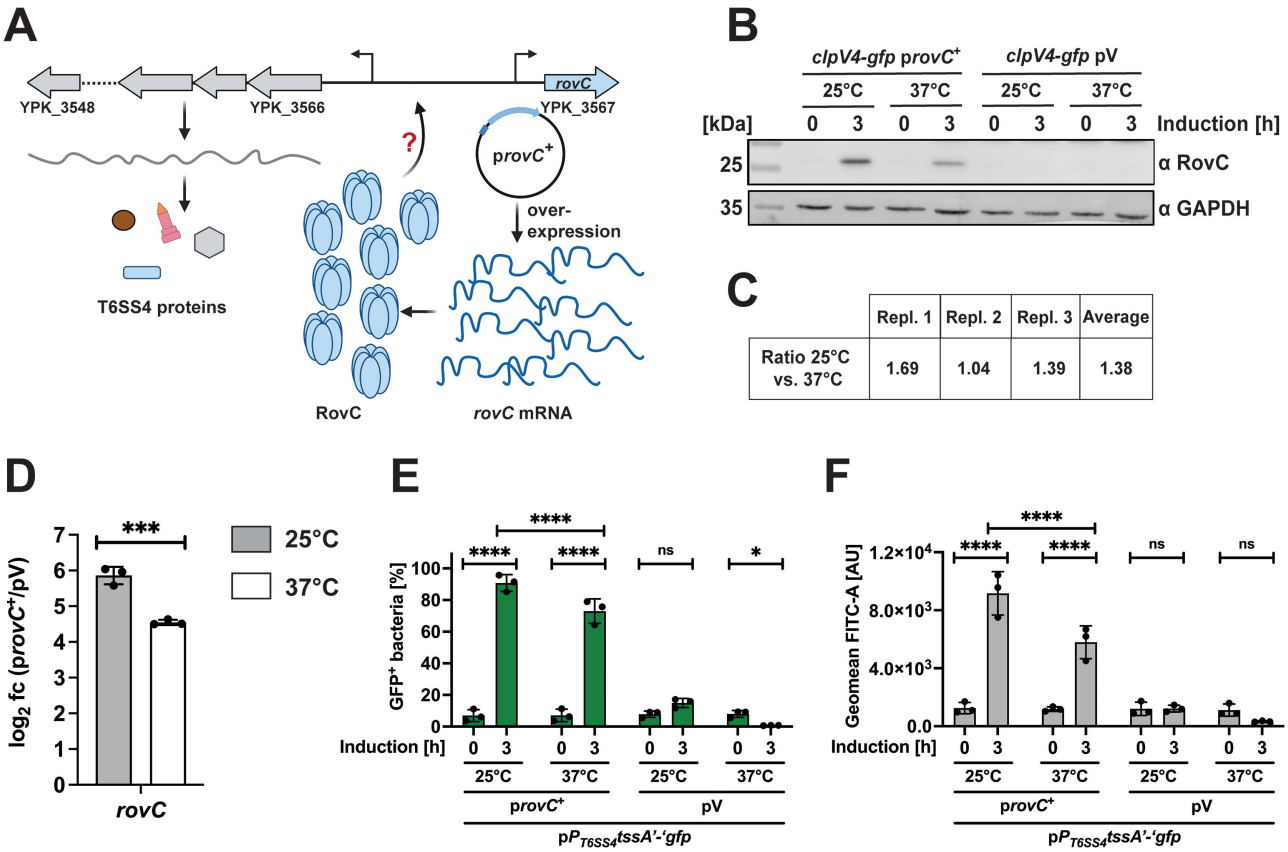

Fig 6. T6SS4 promoter expression can be induced by an overexpression of *rovC* at 37°C. (A) To investigate RovC functionality at 37°C, *rovC* was overexpressed from a non-temperature-sensitive P_{BAD} promoter (P_{BAD} *rovC*, *provC*⁺). Created in BioRender. Dersch, **P.** (2025) https://BioRender.com/vt98mb7. **(B)** Western blotting of wt *clpV4-gfp* harboring P_{BAD} *rovC*⁺ (*provC*⁺) or empty vector (pV) 0 h and 3 h after inducing overexpression of *rovC* at 25°C or 37°C. Protein levels of RovC were detected with a specific antibody against RovC, and GAPDH was used as a loading control. Experiments were performed in three independent replicates; one representative Western blot is shown. **(C)** Ratio of RovC between 25°C and 37°C. The amount of detected RovC of all three Western blot replicates was normalized to the loading control, and the ratio between 25°C and 37°C was calculated. **(D)** Total RNA of samples in (B) was extracted to perform qRT-PCR to determine expression levels of the *rovC* gene. Expression levels were normalized to *sopB* as a non-temperature-regulated reference gene [6] and log2 fold changes 3 h after inducing overexpression of *rovC* between p*provC*⁺ and empty vector control (pV) were calculated. Experiments were performed in three independent replicates. Significant differences were determined using an unpaired t-test. **(E-F)** Promoter region of T6SS4 and first codons of *tssA4* were translationally fused to *gfp* on a plasmid to identify bacteria with an active T6SS4 promoter by flow cytometry. Strains additionally harbored p*provC*⁺ or empty vector (pV), and overexpression of *rovC* was induced for 3 h at either 25°C or 37°C. The amount of GFP⁺ bacteria (E) and the expression intensity (F) of 1×10^5 bacteria were analyzed, and the data depict the mean and standard deviation of three independent experiments. Significant differences were determined using Two-Way ANOVA with Tukey's correction. * = $p \leq 0.05$, *** = $p \leq 0.001$, **** = $p \leq 0.0001$, ns = not significant $p > 0.05$.

https://doi.org/10.1371/journal.ppat.1013356.g006

be identified as T6SS4-ON at 37°C (Fig 7B). This suggests that not only the level of *rovC* mRNA but also that of T6SS4 transcripts is influenced by temperature. A qRT-PCR analysis comparing the transcript levels of five T6SS4 genes (*tssA4, vipA4, hcp4, clpV4,* and *tssK4*) after RovC induction supported this assumption (Fig 7C). The abundance of most transcripts was significantly lower at 37°C compared to 25°C (Fig 7C). One exception is *hcp4,* for which similarly high levels of the *hcp4* transcript and the Hcp4 protein were detected at 25°C and 37°C temperatures (Fig 7C and 7D).

It is unlikely that this expression pattern is caused by an additional promoter located upstream within the T6SS4 operon, as no promoter or an additional transcriptional start site upstream of *hcp4* is predicted [6,18]. Moreover, a translational *hcp4'-'gfp* fusion construct harboring the 5'UTR upstream of *hcp4* without the T6SS4 promoter was not expressed

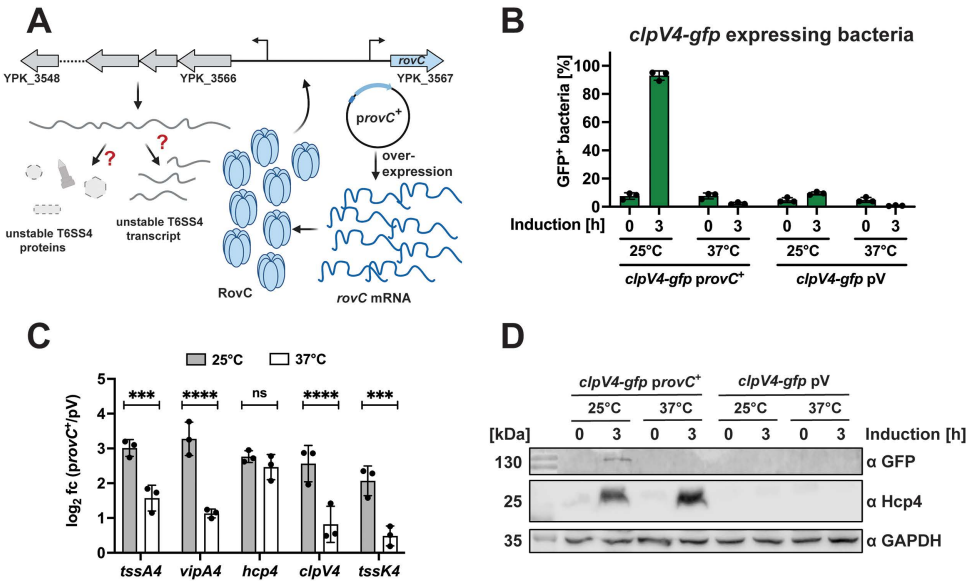

Fig 7. The overall amount of individual T6SS4 gene mRNAs differs significantly at 37°C and 25°C. (A) Scheme of potential downregulation of T6SS4 expression at 37°C caused by an unstable T6SS4 transcript or T6SS4 proteins. Created in BioRender. Dersch, **P.** (2025) https://BioRender.com/947o0tl. **(B)** Quantification of *clpV4-gfp* expressing bacteria after inducing overexpression of *rovC* for 3 h at either 25°C or 37°C. Data depict the mean and standard deviation of three independent experiments. **(C)** Total RNA of samples analyzed in B) was extracted for qRT-PCR. Specific primer pairs for five T6SS4 genes were used to determine gene expression within the T6SS4 operon. All expression levels were normalized to *sopB* as a reference gene, and log2 fold changes 3 h after overexpressing *rovC* between p*rovC*$^+$ and empty vector control (pV) were calculated. Experiments were performed in three independent replicates, and significant differences were determined using a Two-Way ANOVA with Šidák correction. **(D)** Western blotting of the same samples analyzed in **(B)**. Protein levels of ClpV4-GFP and Hcp4 were detected using specific antibodies against GFP and Hcp4. GAPDH was used as a loading control. One representative Western blot out of three independent experiments is shown. * = $p \leq 0.05$, *** = $p \leq 0.001$, **** = $p \leq 0.0001$, ns = not significant $p > 0.05$.

https://doi.org/10.1371/journal.ppat.1013356.g007

(S6 Fig). Taken together, this suggests that in addition to the *rovC* mRNA, the transcripts of the individual T6SS4 genes are post-transcriptionally controlled, but to a different extent.

To prove this, we compared the transcript levels of eight genes covering different regions of the T6SS4 operon under native (non-RovC-inducing) conditions using qRT-PCR (Fig 8A and 8B). We found that the overall abundance of transcripts covering the different genes of the operon varied significantly. The transcript levels of the first four encoded genes in the operon (*tssA4, vipA4, vipB4, hcp4*) were significantly higher compared to the genes further downstream (*tssE4, tssF4*, *clpV4, tssK4*) (Fig 8B). A comparison of the qRT-PCR data with the transcription profile of the individual T6SS4 genes using our RNA-sequencing data supported this observation and confirmed a particularly high abundance of the *hcp4* transcript (S7 Fig).

Subsequent Northern blotting with an *hcp4* probe revealed multiple bands of different sizes, further indicating a processed T6SS4 transcript (Fig 8C). As T6SS4 expression in the *Y. pseudotuberculosis* wt is generally very low, the *csrA* mutant was used for better visualization of the *hcp4* transcript on the Northern blot, as deletion of this global regulator leads to an overall upregulation of T6SS4 gene cluster expression (Figs 4 and S4). A *rovC* mutant strain was used as a negative control, as this abolishes T6SS4 expression [30].

The results strongly suggest that the differences in T6SS4 transcript levels result from post-transcriptional control mechanisms such as differential mRNA degradation, stabilization, and/or transcriptional termination. Secondary structure prediction of the intergenomic region between *hcp4* and *tssE4* revealed a GC-rich stem loop directly downstream of the *hcp4* gene (Fig 8D). The hairpin stem was chromosomally mutated to test whether this loop functions as a potential

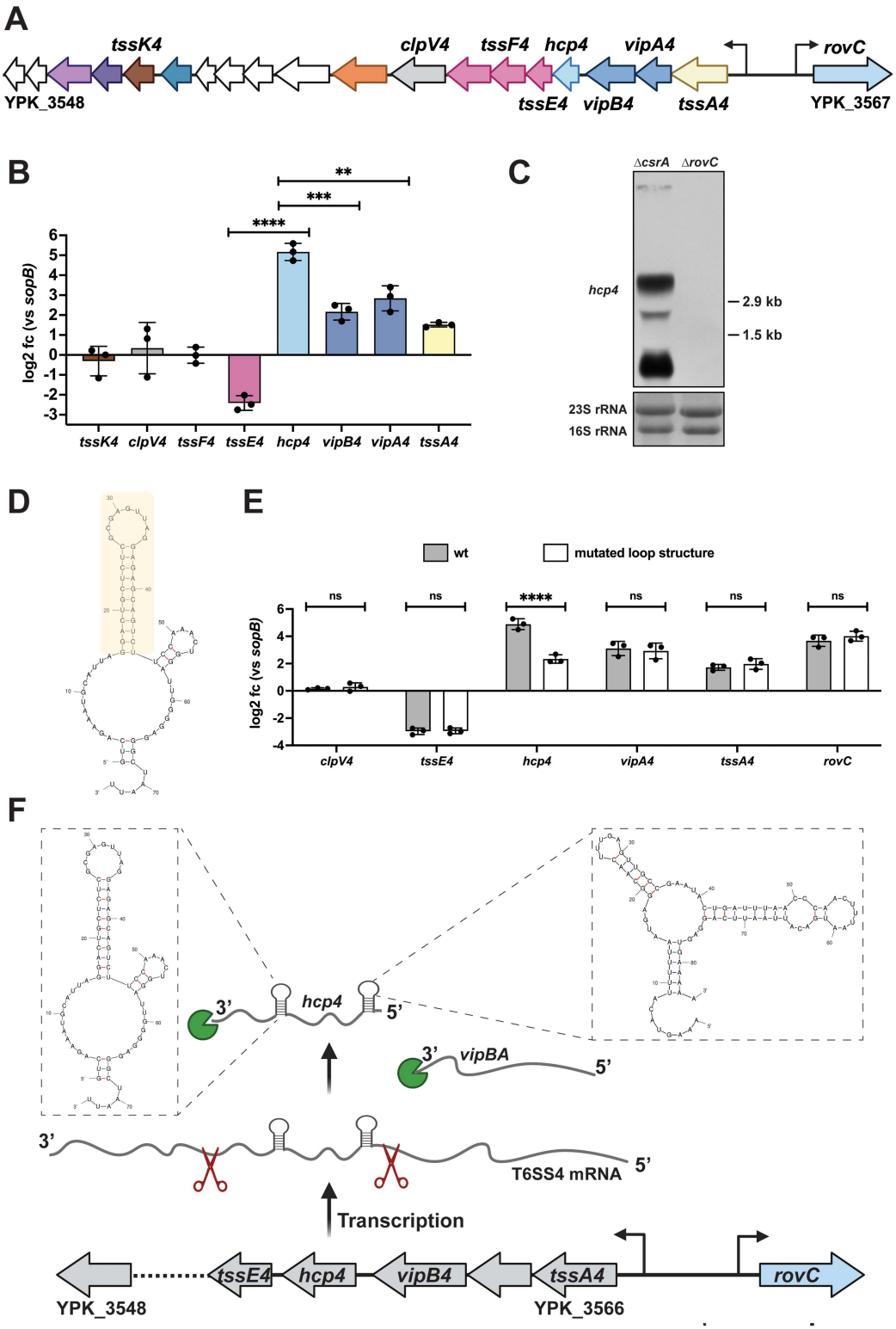

Fig 8. Different abundance of individual T6SS4 gene transcripts. (A) Schematic overview of the T6SS4 operon. **(B)** Total RNA of *Y. pseudotuberculosis* wt incubated for 6 h at 25°C was extracted to perform qRT-PCR. Specific primer pairs for eight T6SS4 genes were used to determine expression levels within the operon, log2 fold changes to *sopB* as a non-temperature-regulated reference gene [6] were calculated. Experiments were performed

in three independent replicates, and significant differences were determined using an unpaired t-test. **(C)** Northern blot of total RNA of YP53 (Δ*csrA*) and YP154 (Δ*rovC*). A specific probe for *hcp4* was used; 16S and 23S rRNA were used as loading controls. **(D)** Secondary structure of the wildtype intergenomic region between *hcp4* and *tssE4* was predicted using the mFold web server [65]. The region which was mutated is marked in yellow. **(E)** Total RNA of *Y. pseudotuberculosis* wt and a strain with the mutated loop structure grown for 6 h at 25°C was extracted to perform qRT-PCR. Specific primer pairs for six T6SS4 genes were used to determine expression levels within the operon, and log2 fold changes to *sopB* as a non-temperature-regulated reference gene [6] were calculated. Experiments were performed in three independent replicates, and significant differences were determined using a Two-Way ANOVA with Šidák correction. **(F)** Scheme of potential post-transcriptional T6SS4 regulation. The T6SS4 transcript is processed due to endoribonucleolytic cleavage (red scissors). The 5' and 3' protection loop up- and downstream of *hcp4* protects the *hcp4* transcript from further endonuclease activity and from being degraded by exoribonucleases (green pie). The loop structures of the 5'-UTR and 3'-UTR of *hcp4* were predicted using the mFold web server [65]. Created in BioRender. Dersch, **P.** (2025) https://BioRender.com/efeis70. ** = p ≤ 0.01, *** = p ≤ 0.001, **** = p ≤ 0.0001, ns = not significant p > 0.05.

https://doi.org/10.1371/journal.ppat.1013356.g008

transcription terminator, which would explain the observed transcriptional stop after *hcp4* (Fig 8D, marked in orange). qRT-PCR revealed no differences in the transcript levels of the tested T6SS4 genes (Fig 8E). Only the transcript level for *hcp4* was significantly reduced in the strain with the mutated stem loop compared to wt. This indicates that the loop may not function as a transcriptional terminator to pause transcription downstream of *hcp4*, but rather acts as a 3'-protective loop to resist exoribonucleolytic degradation of *hcp4* mRNA after endolytic cleavage at this site (Fig 8F). The inspection of the T6SS4 cluster further revealed another potential stem-loop structure that could be formed in the intergenic region between *vipB4* and *hcp4* (Fig 8F). The intergenomic region additionally consists of several AUUA-motifs, which could be recognized and then cleaved by endoribonucleases. As the *hcp4* probe interacted with a small RNA fragment of the expected size of the *hcp4* gene of around 500 bp (Fig 8C), it is likely that this stem-loop structure also contributes to processing and/or stabilization of the *hcp4* transcript.

Discussion

Y. pseudotuberculosis is a widespread environmental bacterium that can also infect mammals [1,2]. This dual lifestyle requires a precise and rapid change in gene expression in response to changing conditions, such as entry into the human body. In this context, temperature plays an important role in the regulation of gene expression in *Y. pseudotuberculosis*, since many virulence-associated and metabolic genes are strictly controlled by temperature [5,6]. In this study, we could show that the T6SS4 in *Y. pseudotuberculosis* is strongly regulated by temperature but in the opposite manner to the T3SS. At moderate temperatures (25°C), the T6SS4 gene cluster is heterogeneously expressed, with only 10–15% of the population producing the transcriptional regulator RovC at levels which are sufficient to induce T6SS4 expression. At 37°C, *rovC* is rapidly downregulated on post-transcriptional level, leading to a rapid and complete shut-off of T6SS4 gene expression. Moreover, T6SS4 is part of a complex regulatory network that is embedded in global regulation. We found that global regulators such as the carbon starvation system regulator CsrA, the global protease Lon, the *Yersinia* modulator protein YmoA, and the two RNases PNPase and RNase III repress RovC and T6SS4 synthesis at 25°C. This indicated a very sophisticated and tight control of T6SS4 gene expression in response to temperature and other environmental signals that differs fundamentally from the control of T6SS expression in other bacteria.

In this study, a deeper analysis of T6SS4 expression showed that differential expression levels of the *Yersinia*-specific transcriptional activator RovC drive T6SS4 heterogeneity (T6SS4-ON versus T6SS4-OFF) (Figs 1 and 2). Phenotypic heterogeneity has been intensively studied in recent years and can be triggered, for example, by microenvironments with different demands, leading to different gene expression within a subpopulation [66,67]. Phenotypic heterogeneity can also be a strategy to survive sudden environmental fluctuations. In this so-called bet-hedging strategy, only some bacteria express certain genes that are not necessary under normal conditions. This additional expression of non-required genes can cost energy and resources. Nevertheless, since no adaptation phase is necessary in the event of sudden changes, the survival of at least a subpopulation is ensured [68–72]. Such bistability of gene expression has been demonstrated for *rovA* in *Y. pseudotuberculosis* controlling invasin expression in response to temperature [73–75]. RovA undergoes a

conformational change upon an upshift from 25°C to 37°C that increases its accessibility for proteases, and hence, its rapid degradation abolishes its positive autoregulation (positive feedback loop) [73–75]. The exact mechanism of how heterogeneity of *rovC* and thus, T6SS4 expression is achieved is still unclear. However, no autoregulation or -activation of RovC was detectable [30], indicating a substantially different mechanism from RovA. Moreover, the functional role of T6SS4 remains unknown. However, the presence of four different T6SS clusters in *Y. pseudotuberculosis* likely requires tight regulation to ensure that T6SS4 expression is restricted to the environments where it is most advantageous.

In contrast to *Y. pseudotuberculosis*, T6SS is not heterogeneously but equally expressed in most studied bacteria, including *Vibrio* and *Pseudomonas,* where the secretion system genes have been extensively studied [19,22,23,26,48–50]. Only one recent study in enteroaggregative *E. coli* (EAEC) has reported that its T6SS is ON in 60% and OFF in 40% of the bacteria [76]. Yet, the implicated regulatory factors in EAEC are very distinct from *Y. pseudotuberculosis.* They found that heterogeneous T6SS expression in EAEC is regulated by the interaction of Fur (ferric uptake regulator) with the T6SS promoter region and genetically controlled by GATC methylation sites [76]. In contrast, heterogeneous T6SS4 expression in *Y. pseudotuberculosis* is already determined by the heterogeneous expression of the transcriptional regulator RovC (Fig 2). In addition, neither Fur binding sites nor GATC methylation sites have been found for RovC, suggesting a different regulation of heterogeneous T6SS4 expression *in Y. pseudotuberculosis*.

Our study further showed that RovC synthesis is the major control hub for T6SS4 expression. All global regulators of T6SS4 and temperature changes seem to influence *rovC* transcript levels strongly but do not affect its promoter activity or protein stability. Several regulatory scenarios are possible. For instance, differential folding of the mRNA in response to temperature could expose or hide RNase cleavage sites [77,78] and/or influence translation efficiency [77,79–85]. Alternatively, the synthesis or activity of RNases targeting the *rovC* mRNA could be increased at higher temperatures, leading to degradation of the *rovC* transcript.

Like other functionally linked genes, all core components of T6SS4 are encoded in close proximity under the control of only one promoter and form a polycistronic mRNA [18]. As a result, only one mRNA is transcribed, which, in theory, should lead to stoichiometrically equal amounts of transcripts. However, not all components are needed to the same extent, and regulatory measures are implemented to adjust T6SS4 component synthesis to their functional need. In the case of the T6SS, for example, proteins that assemble the membrane or the base plate complex are required in lower quantities than those building the tubular structure, which consists of hundreds of copies of stacked Hcp proteins [21,86]. While different translation efficiencies have been described to resolve this problem in some cases [87,88], we show that T6SS4 gene expression differences have already occurred at the transcript level. Very low transcript levels were detected for the genes downstream of *hcp4.* In contrast*,* the mRNA abundance of the first four genes of the operon was significantly higher, particularly *hcp4*, encoding the tube protein. No additional promoter activity was detected upstream of *hcp4* (S6 Fig), and no other additional transcriptional start site within the operon has been identified [6,18]. Thus, differential T6SS4 mRNA levels seem to result from endoribonucleolytic cleavage of the polycistronic T6SS4 cluster mRNA at two sites with stem-loop structures flanking the *hcp4* gene. A very rapid exoribonucleolytic degradation can explain the low abundance of the T6SS gene transcripts downstream of *hcp4*. In contrast, both stem loops flanking the resulting short *hcp4* transcript will likely protect the transcript from further cleavage, leading to very high *hcp4* transcript and thus Hcp4 protein levels (Figs 8C and 5D). Differential processing and degradation of polycistronic mRNA are described for several bacterial operons [77,89–93]. Processing of polycistronic mRNAs, resulting in stabilization of upstream genes (*e.g.,* by the presence of stem loop structures, as identified downstream of *hcp4*) was described for the maltose and *iscRSUA* operon in *E. coli* or the *puf* operon in *Rhodobacter capsulatus* [77,89,90,94]. Endonucleolytic cleavage of mRNAs can also lead to a lower abundance of upstream transcripts (as observed for *tssA4*, *vipA4, vipB4*, compared to *hcp4*) due to degradation by 3'-5'-exoribonucleases. Such a mechanism has been demonstrated for the *pap* and glycogen operon in *E. coli* [77,91,92,95]. Alternatively, as reported in other systems [89,96,97], strong translation of the *hcp4* gene could prevent this gene from being degraded by 3'-5' exoribonucleases.

The observed post-transcriptional regulation of the T6SS4 polycistron, leading to a different abundance of T6SS4 transcripts, fits with studies reporting differential T6SS protein amounts [86]. Some proteins, such as those coding for the baseplate, require only a small number of copies, whereas the tube and sheath structure components require many copies [21,29,52,98–100]. After a firing event, the sheath structure components VipA and VipB are disassembled by the ATPase ClpV and remain in the cell [29,49,101,102]. In contrast, Hcp is secreted with VgrG and the effector proteins into the target organism and can be found in the supernatant after a firing event [21,26,103,104]. This requires immediate *de novo* synthesis of the secreted proteins in case of a new firing event. To solve this, other organisms such as *Vibrio spp*. encode, in addition to the main T6SS island, auxiliary clusters with *hcp* or effector proteins under the control of a separate promoter [20,50,105,106]. Since a single promoter controls all T6SS4 genes in *Y. pseudotuberculosis*, the observed differential stabilization of the respective mRNAs is an effective way for *Y. pseudotuberculosis* to meet the different protein requirements.

To date, the precise role of T6SS4 is still unclear. The highest expression of *rovC* and T6SS4 at moderate temperatures and their strong repression at 37°C observed in this and other studies (Figs 1C and 5A, [18,31]) indicate a function outside mammalian hosts. This is supported by multiple RNA sequencing datasets, including an *in vivo* transcription profile of *Y. pseudotuberculosis* within the Peyer's patches during a mouse infection [6,44,46,47], revealing a complete repression of T6SS4 gene expression at body temperature. Most interestingly, we found T6SS4-type clusters in the environmental-associated strains *Winslowiella toletana, Serratia fonticlola, Enterobacillus tribolii, Trabulsiella guamensis, T. odontotermitis,* which belong to the family of *Enterobacteriaceae* (Fig 9). The identified T6SS clusters are homologous in synteny and protein identity to the T6SS4 of *Y. pseudotuberculosis* and T6SS-A of *Y. pestis.* Among them, *W. toletana* shows the highest protein identity to the T6SS4 of *Y. pseudotuberculosis,* including the gene of the so far unique transcriptional activator RovC (Fig 9, > 70% amino acid identity). Initially described as *Erwinia toletana*, *W. toletana* exhibits an optimal growth temperature between 28°C and 30°C [107,108]. It was first isolated from olive knots in association with the plant pathogen *P. savastanoi*, and its presence has been shown to enhance olive tree infection [107,109]. *T. guamensis* was found in soil, vacuum cleaner dust, or human stool samples, *T. odontotermitis* and *E. tribolii* were isolated from the gut of termites and red fluor beetle, respectively [110–113]. *S. fonticola* is a widely distributed environmental bacterium, commonly found

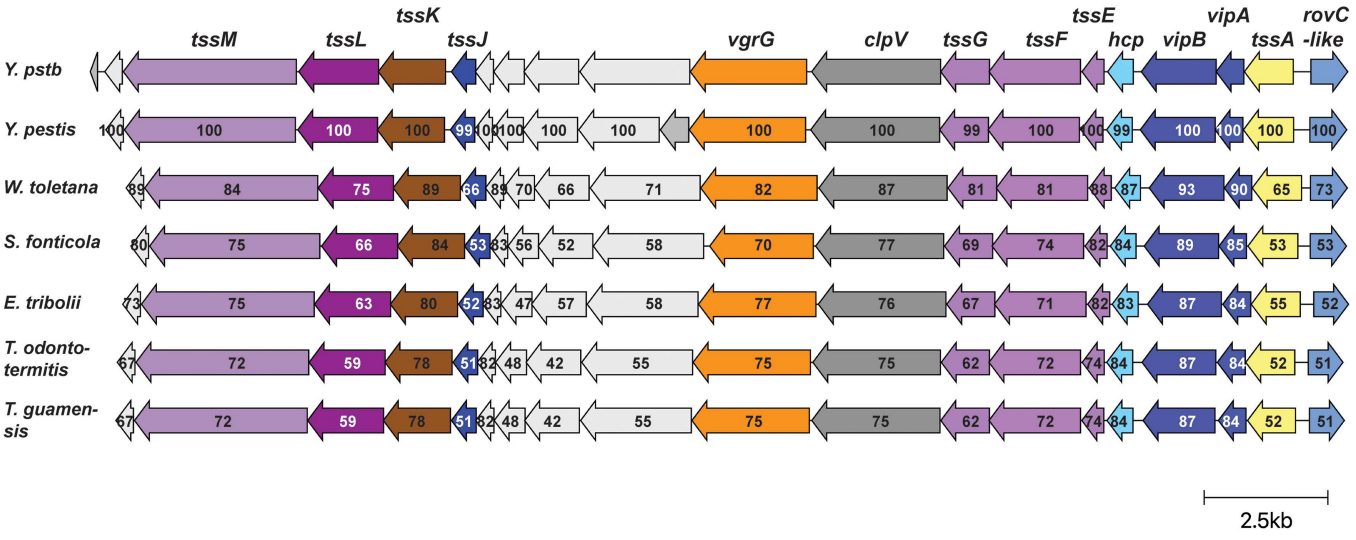

Fig 9. Identification of homologous T6SS4 cluster in different *Enterobacteriaceae*. The amino acid identity of T6SS4 components between *Y. pseudotuberculosis* and different strains is given as a percentage based on protein sequence similarity. Visualization of the cluster similarities was done using clinker webserver [117]. The scale bar represents 2.5 kb.

https://doi.org/10.1371/journal.ppat.1013356.g009

in soil or aquatic habitats [114,115]. Despite a few clinical cases of *S. fonticola*, none of the organisms are considered primary human pathogens. The high amino acid identity, particularly for *W. toletana* strongly indicates a similar function of the T6SSs, possibly linked to a plant- or insect-associated ecological niche [116].

In contrast to these assumptions, one group reported that some potential T6SS4 effectors are essential for virulence in mice [40,42,43]. One of these potential effectors (YPK_3548) is encoded at the 3'-end of the T6SS4 cluster. This gene is however not present in the T6SS4-type cluster in *Y. pestis* and *W. toletana* (Fig 9), and its expression was not affected by the loss of the *csrA* gene, in contrast to all other T6SS4 cluster genes [30]. As all *in vitro* experiments to characterize the effectors were also carried out at 26°C [40,43], a more detailed analysis of the *in vivo* function of the T6SS4 system and its putative effectors is required to elucidate whether the T6SS4 system is important for a plant- and/or animal-associated lifestyle.

Materials and methods

Media and growth conditions

E. coli was grown overnight in 5 ml Luria-Bertani (LB) medium (5 g/l yeast extract, 10 g/l tryptone, 5 g/l NaCl) at 37°C. Super Optimal Broth with Catabolic Repression (SOC) medium (5 g/l yeast extract, 20 g/l tryptone, 10 mM NaCl, 2.5 ml KCl, 10 mM $MgSO_4$, 10 mM $MgCl_2$, 20 mM glucose) was used to allow *E. coli* cells to recover after transformation. The medium is based on Super Optimal Broth (SOB) medium [118], supplemented with glucose. *Y. pseudotuberculosis* was grown in LB (BD Bioscience, USA), supplemented with 1 mM $CaCl_2$ or in brain-heart infusion (BHI) medium (37 g/l BHI, BD Bioscience, USA). Unless stated otherwise, *Y. pseudotuberculosis* cultures were incubated overnight at 25°C in LB, main cultures at either 25°C or 37°C. If necessary, selective antibiotics were added in the following final concentration: 100 µg/ml ampicillin, 50 µg/ml kanamycin, and/or 50 µg/ml chloramphenicol. To induce overexpression of *rovC* from pBAD30 plasmid, 0.1% arabinose was added to the culture in early exponential phase (OD_{600} 0.7).

Plasmid and strain construction

In this study, molecular cloning of DNA into vectors was performed following the Gibson Assembly Protocol (E5510) (New England Biolabs), based on the method developed by Gibson *et al*. [119]. Plasmid DNA was isolated using the Nucleospin Plasmid kit (Macherey Nagel), and genomic DNA of *Y. pseudotuberculosis* was isolated using the ISOLATE II Genomic DNA Kit (Bioline). The oligonucleotides used for cloning, sequencing and qRT-PCR were purchased from Eurofins Genomic. PCRs for fragment amplification were performed using Q5 High-Fidelity 2X Master Mix (New England Biolabs) following the manufacturer's instructions. PCR products were purified using Nucleospin Gel and PCR clean-up kit (Macherey Nagel). To verify correct clones, colony PCRs were performed using 2x DreamTaq Green PCR Master Mix (Thermo Scientific) according to the manufacturer's instructions. Sanger sequencing (Microsynth Seqlab GmbH) confirmed successful cloning of plasmids. Plasmids and primers used in this study are listed in S1 and S2 Tables.

For cloning of pANK4 and pANK15, vector pFU98 was linearized by digestion with *Nhe*I and *Not*I (New England Biolabs, Ipswich, USA). For pANK4, the 5'-UTR of *rovC* (-579 to +13) was amplified with primers IX691/692 using Q5 High-Fidelity 2X Master Mix (New England Biolabs). Primers IX687/IX688 were used to amplify *mCherry*. A splicing by overlap extension PCR (SOE PCR) [120] was performed to generate a combined DNA fragment of 5'-UTR of *rovC* and *mCherry*. The combined DNA fragment was cloned into linearized pFU98 following the Gibson Assembly Protocol (E5510) (New England Biolabs). For generating pANK15, primers X108/X109 were used to amplify the 5'-UTR of YPK_3566, including the predicted promoter region of T6SS4 (-581 to +15) [18]. Primers X110/111 were used to amplify *gfpmut3.1*. SOE PCR was performed to generate the combined DNA fragment with primers X108/X111, which was subsequently cloned into linearized pFU98. For cloning of pANK25, vector pFU31 was linearized with *Sal*I and *Nhe*I (New England Biolabs, Ipswich, USA). The 5'UTR of *hcp4* (-212 to +30) was amplified with primers X382/X383. The amplified DNA fragment was subsequently cloned into linearized pFU31. For cloning of pANK45, the suicide plasmid pAKH3 was linearized by

digestion with *Xma*I and *Sph*I (New England Biolabs, Ipswich, USA). The upstream and downstream region of the intergenomic region between *hcp4* (YPK_3563) and *tssE4* (YPK_3564) were amplified with primers X558/X559 and X560/X561, respectively. A combined DNA fragment of the upstream and downstream region was generated with primers X558/X561 performing a SOE PCR.

All generated vectors were transformed into electrocompetent *E. coli* SM10 λpir. 500 ml of LB were inoculated 1:100 with an *E. coli* overnight culture and grown to an OD_{600} of 0.6 at 37°C. The culture was pelleted for 10 min at 8,000x g and 4°C, followed by two washing steps with 50 ml and 25 ml ice-cold water. After an additional washing step in 1 ml ice-cold water, the cells were centrifuged again for 10 min at 8,000 x g and 4°C. The pellet was resuspended in a final volume of 1.8 ml ice-cold 10% glycerol. 50 µl aliquots were immediately frozen in liquid nitrogen and stored at -80°C. For transformation, 2 µl of plasmid DNA was added to 50 µl competent cells and exposed to 2.2 kV (200 Ω, 25 µF) for 5 ms in a pre-cooled electroporation cuvette. Transformed *E. coli* cells were mixed with 1 ml SOC and incubated for 1 h at 37°C with permanent aeration to recover. Afterwards, the cells were pelleted for 2 min at 8,000 x g, resuspended in 100 µl medium, plated out, and incubated overnight at 37°C on agar plates with the desired antibiotic. Correct cloning of generated plasmids was confirmed by Sanger sequencing.

Electrocompetent *Y. pseudotuberculosis* strains were used to transform pVK25, pBAD30, pANK4, pANK15, pANK25, pFU31, pKD4, and pCP20. The 15 ml BHI medium was inoculated 1:50 with *Y. pseudotuberculosis* overnight cultures. After 3 h of incubation at 25°C, the culture was pelleted for 5 min at 8,000 x g and 4°C and washed twice with 5 ml ice-cold sterile water. After the second wash, the pellet was resuspended in 200 µl ice-cold water and immediately used for transformation. For each transformation, 2 µl plasmid DNA and a 50 µl aliquot of competent cells were added to a pre-cooled electroporation cuvette. Transformation was performed by exposing the cells for 5 ms to 2.2 kV (200 Ω, 25 µF). Subsequently, the transformed cells were allowed to recover in 1 ml BHI medium for 2 h at 25°C under constant aeration. 100 µl of each transformation was plated on agar plates with the corresponding antibiotics and incubated at 25°C for two days.

Construction of *Y. pseudotuberculosis* mutants

All strains used in this study are listed in S1 Table. Chromosomal *Y. pseudotuberculosis* mutants were generated by homologous recombination using suicide plasmids derived from pAKH3 [121], except for YP78. For chromosomal fusion of *clpV4* to *gfp,* pASS90 was conjugated into the respective *Y. pseudotuberculosis* strains. For chromosomal deletion of the intergenomic region between *hcp4* and *tssE4*, pANK45 was conjugated into *Y. pseudotuberculosis* wildtype [122]. Conjugation of *Y. pseudotuberculosis* was followed by sucrose selection on agar plates containing 6% sucrose. After conjugation, correct clones were confirmed by PCR and Sanger sequencing (Microsynth Seqlab GmbH).

To chromosomally delete *lon* (YPK_3232), a Red-mediated recombination method was used as described [123]. In brief, primers I407/I408 were used to amplify a kanamycin resistance cassette with homologous regions of YPK_3232 using pKD4 as template. The amplified DNA fragment was transformed into YPIII harboring pKD4. Loss of pKD4 and successful gene disruption were confirmed with colony PCR. The kanamycin resistance cassette was eliminated by transformation of the mutated strain with pCP20. Afterwards, the plasmid was cured by incubating for 3h at 42°C due to the temperature-sensitive replicon [123,124].

Fluorescence-based flow cytometry

Flow cytometry was performed as a high-throughput method to analyze gene expression and promoter activity using the CytoFLEX S (Beckmann Coulter, USA). To avoid the detection of spillover signal, a compensation matrix was applied for all used fluorochromes according to the manufacturer's manual. To separate bacteria from the debris, the samples were stained with 5 µg/ml 4′,6-diamidino-2-phenylindole (DAPI) and detected by the PB450 channel. The ECD channel was used to differentiate live and dead cells, which were stained with 1 µg/ml propidium iodide (PI). FITC was used to detect GFP-expressing bacteria. In experiments, where *rovC* promoter activity was analyzed

by gating for mCherry$^+$ bacteria, the samples were not stained with PI, and mCherry$^+$ bacteria were analyzed in the ECD channel. The threshold was set to 2500, defined by sideward scatter height (SSC-H). In this study, the gain for the SSC was set to 400, for the forward scatter (FCS) to 100, for PB450–300, for ECD to 1250, and for fluorescein isothiocyanate (FITC) to 700. For the analysis of GFP- or mCherry-expressing bacteria, the samples were incubated according to the respective experiment. Depending on the OD_{600}, 1–10 µl were taken directly from the culture at indicated timepoints and added to 500 µl PBS with 5 µg/ml DAPI and 1 µg/ml PI. 1 x 10^5 bacteria were analyzed for every sample using the gating strategy displayed in S2 Fig.

Fluorescence microscopy

Fluorescence microscopy was performed using the Keyence epi-fluorescence microscope BZ-X (Osaka, Japan) at 60x magnification (Plan Apochromat 60x Oil). The samples were pelleted for 5 min at 8,000x g at room temperature and resuspended to an OD_{600} of 10. From this dense suspension, 1 µl was transferred to an agarose pad containing 1% agarose and 0.5 x PBS to avoid the swimming of motile *Y. pseudotuberculosis*. For an even surface, the agarose was poured on a microscopy slide, fitted with a gene frame (Thermo Fisher Scientific, Waltham, USA).

RNA isolation

Bacterial cultures were grown according to the respective experiment. At indicated timepoints, 2 ml of the culture were pelleted for 2 min at 10,000x g at room temperature. The pellet was directly frozen in liquid nitrogen and stored at -80 °C until isolation of total RNA. Total RNA was extracted using the Monarch Total RNA Miniprep Kit (New England Biolabs) according to the manufacturer's protocol: "Total RNA Purification from Tough-to-Lyse Samples (bacteria, yeast, plant, etc.)". The first part of the sample digestion and homogenization protocol was modified as follows: After thawing, the bacterial pellet was resuspended in 200 µl TE-buffer (100 mM Tris HCl pH 7.5, 1 mM EDTA pH 8) containing 10 mg/ml lysozyme (L6876, Sigma-Aldrich) and incubated for 10 min at room temperature. Afterwards, 2x volumes RNA Lysis Buffer were added and the sample was vortexed vigorously for 10 sec. After centrifugation for 2 min at 16,000x g, the supernatant was transferred to a gDNA removal column. The extraction was proceeded with the second part of the RNA Binding and Elution protocol. Total RNA was diluted with 50 µl of nuclease-free water, and the purity and concentration were determined using the Nanodrop spectrophotometer (Thermo Fisher Scientific, Waltham, USA). Because of the high abundance of genomic DNA, an additional DNA digestion step was included after isolation of total RNA. For this, 7.5 µg RNA was filled up to 44 µl of nuclease-free water, 5 µl 10X TURBO DNase buffer, and 1 µl TURBO DNase enzyme (Invitrogen, Thermo Fisher Scientific, Waltham, USA). Samples were incubated for 30 min at 37°C, followed by adding 1 µl of TURBO DNase enzyme and incubating for 30 min at 37°C. The reaction was stopped by adding 5 µl DNase Inactivation Reagent (Invitrogen, Thermo Fisher Scientific, Waltham, USA). After inactivation, the sample was centrifuged for 3 min at 16,000 x g at room temperature, and 35 µl were transferred to a fresh reaction tube. Purity and concentration of the RNA were again analyzed using the Nanodrop spectrophotometer, and the RNA was diluted to 15 ng/µl and stored at -80°C for further experiments.

Quantitative real-time PCR (qRT-PCR)

To determine the amount of transcript of different T6SS4 genes, qRT-PCR was performed using the Luna Universal One-Step RT-qPCR Kit (New England Biolabs) with the LightCycler 96 System (Roche). Each reaction was performed in technical triplicates in a 10 µl reaction, containing 5 µl Luna Universal One-Step Reaction Mix (2x), 0.5 µl Luna WarmStart RT Enzyme Mix (20x), 0.5 µl of each primer (10 µM) and 1 µl of the desired RNA template (15 ng/µl). The reaction was filled up with nuclease-free water to 10 µl. Relative changes in gene expression were calculated using *sopB* as a reference gene [6,125]. Primers used for qRT-PCR are listed in S2 Table.

Northern blot

In order to detect the *hcp4* transcript, a DIG-labelled *hcp4*-specific probe was generated (Primers are listed S2 Table). Total RNA was isolated, and 15 µg/20 µl of RNA was used for the Northern blot. The samples were mixed with 4 µl of 5x loading dye (31% formamide, 2.7% formaldehyde, 0.1 mg/ml ethidium bromide, 4 mM EDTA pH 8, 20% glycerol, 0.03% bromphenole blue, 10% MOPS buffer (20x)). The samples were boiled 2x for 10 min at 70°C with 5 min in between at 10°C. The samples were immediately incubated for 2 min on ice before they were separated on a MOPS agarose gel containing 1.2 g agarose, 5.5 ml 20% MOPS buffer (400 mM MOPS, 100 mM sodium acetate, 20 mM EDTA) and filled up to 100 ml distilled water. After the separation, the 16 and 23S rRNA loading control were detected using UV-light. To transfer the RNA on a positively charged nylon membrane, vacuum blotting was carried out for 1.5 h and 5 bars. After UV-crosslinking of the membrane, the membrane was prehybridized for 1 h at 42°C in prehybridization buffer containing 20 ml formamide, 10 ml 20x SSC buffer (3 M NaCl and 0.3 M NaCitrate, pH 7), 8 ml 10x blocking agent (Roche Blocking reagent), 2 ml N-Laurylsarcosinate (20 mg/ml), 40 µl 20x SDS, and 2 ml distilled water. 3 µl of the DIG-labelled DNA probe was added to 200 µl water, heated (10 min, 95°C), and cooled down (5 min on ice) twice a row. After a final heating to 95°C for 10 min, the probe was directly added to 20 ml prehybridization buffer. The nylon membrane was incubated and hybridized with the DNA probe overnight at 42°C. Next, the membrane was washed twice for 5 min at room temperature with washing buffer 1 (0.2x SSC buffer, 0.1% SDS) followed by an additional washing step for 15 min at 68°C with washing buffer 2 (0.1x SSC buffer, 0.1% SDS). The membrane was then blocked for 1 h at room temperature in 1x blocking reagent (Roche Blocking reagent) in maleic acid buffer. To visualize the *hcp4* transcript, the membrane was incubated for 1.5 h with a α-Digoxygenin antibody (Anti-Digoxigenin-AP (fab fragments), Roche) 1:6000 in 1x blocking agent in maleic acid buffer. After the incubation with the antibody, the membrane was washed twice for 15 min each at room temperature with CPD* washing buffer (0.1 M maleic acid, 0.15 M NaCl, 0.3% TWEEN-20, pH 7.5). Washing of the membrane was subsequently followed by equilibration for 5 min in the detection buffer (0.1 M Tris-HCl pH 9.5, 0.1 M NaCl). To finally detect the hybridized probe, the membrane was incubated for 5 min with 1 ml of the substrate solution (1:100 CDP* (CDP-Star system, Roche) in detection buffer). The signal was recorded via exposure on X-ray films (CL-Xposure, Thermo Scientific, USA).

Western blot

For the detection of RovC, Hcp4 and ClpV4-GFP proteins, cultures were incubated depending on the desired conditions. At indicated timepoints, whole cell extracts were prepared by pelleting 1 ml of each sample for 5 min at 8,000x g at RT. The pellet was resuspended in an adjusted 1x Laemmli buffer [126] (40% v/v glycerol, 240 mM Tris-HCl, 8% w/v SDS, 5% v/v β-mercaptoethanol and 0.04% w/v bromophenol blue) to an OD_{600} of 10 and heated for 10 min at 95°C. Proteins were separated on a 15% polyacrylamide gel and transferred onto a polyvinylidene fluoride (PVDF) membrane (Sigma) by Western blotting. Primary antibodies against RovC (1:1000 dilution) and Hcp4 (1:5000) were generated by Davids Biotechnology, ClpV4-GFP was visualized using a monoclonal antibody against GFP (#MAB 3580, Merck Millipore, 1:2000). GAPDH was used as loading control and visualized with a monoclonal antibody against bacterial GAPDH (#MA5–15738, Invitrogen, 1:2000).

β-galactosidase assays

The β-galactosidase assay, first described by Miller 1972 [127], was used to determine *rovC* promoter activity. *Y. pseudotuberculosis* strains harbored pAKH189 or pTS03, respectively were incubated at 25°C and 37°C. At indicated timepoints, 200 µl samples were permeabilized by adding 50 µl 0.1% SDS and chloroform, respectively. After incubation for 10 min, 1.8 ml Z-buffer was added (60 mM Na_2HPO_4, 20 mM NaH_2PO_4, 10 mM KCl, 1 mM $MgSO_4$). The reaction was started by adding 400 µl ONPG as substrate (4 mg/ml). The reaction was stopped by adding 1 ml of 1 M Na_2CO_3. The activities were calculated as follows: ß-galactosidase activity [Miller units] = $1000 \times OD_{450} \times \Delta t\ (min)^{-1} \times V\ (ml)^{-1} \times OD_{600}$.

Supporting information

S1 Table. Bacterial strains and plasmids.
(DOCX)

S2 Table. Oligonucleotides for DNA amplification.
(DOCX)

S1 Fig. *clpV4-gfp* expression is repressed at 37°C. Fluorescence microscopy of *Y. pseudotuberculosis* wt *clpV4-gfp* incubated for two and 6 h at 25°C (A) or 37°C (B). Representative images of the brightfield and GFP channels and an overlay of both channels were shown. Bacteria were imaged on agarose pads containing 1% agarose, and the scale bar represents 10 μm.
(TIF)

S2 Fig. Gating strategy to analyze heterogeneous T6SS4 and *rovC* expression. (A) Samples were stained with DAPI to gate for bacteria. (B) PI staining to exclude dead bacteria. (C) Negative control (YPIII wildtype) for GFP-expressing bacteria. (D) Gate for GFP-expressing bacteria. (E) Negative control (YPIII wildtype) for mCherry-expressing bacteria. (F) Gates for mCherry-expressing bacteria, divided into low and high expression intensity. H = height, A = area, SSC = side scatter. Exemplary plots are shown.
(TIF)

S3 Fig. Deletion of *lon* results in increased *rovC* promoter activity. Wt *clpV4-gfp* pP_{rovC} *rovC'-'mCherry* and Δ*lon clpV4-gfp* p pP_{rovC} *rovC'-'mCherry* were incubated overnight at 25°C. 1 x 10^5 bacteria were analyzed with flow cytometry, and experiments were performed in four independent experiments. Statistical significance was tested with an unpaired t-test. ns = not significant $p > 0.05$.
(TIF)

S4 Fig. T6SS4 gene expression is downregulated at 37°C. (A-C) Total RNA of an overnight culture of wt, Δ*csrA,* and Δ*ymoA* was isolated to perform qRT-PCR. Specific primer pairs for five T6SS4 genes were used to determine the expression within the T6SS4 operon. Log2-fold changes were calculated between the T6SS4 transcript and *sopB* as a non-temperature-regulated reference gene [6]. Experiments were performed in three biological replicates, and significant differences were determined using a Two-Way ANOVA with Šidák correction **** = $p \leq 0.0001$.
(TIF)

S5 Fig. The *rovC* promoter activity is not subject to temperature-dependent control. Fluorescence microscopy of *Y. pseudotuberculosis* wt *clpV4-gfp* harboring *p*P_{rovC}*rovC'-'mCherry*. Strains were incubated for 2 h and 6 h at either 25°C (A) or 37°C (B). Representative images of the GFP and mCherry channels, overlays of the GFP and mCherry channels, and an overlay of all channels with the brightfield, were shown. Bacteria were imaged on agarose pads containing 1% agarose, and the scale bar represents 10 μm.
(TIF)

S6 Fig. Accumulation of *hcp4* transcript is not due to an additional *hcp4* promoter. A low copy plasmid harboring the upstream region of *hcp4*, p*hcp4'-'gfp* (-212 to +30 base pairs with respect to the translational start site) was transformed into YPIII wt. Samples were incubated in 20 ml LB overnight at 25°C. wt *clpV4-gfp* was used as a control to compare the amount of *clpV4-gfp* expressing bacteria to the potential *hcp4* promoter activity. Samples were taken for flow cytometry, and 1 x 10^5 cells were analyzed. Experiments were performed in three biological replicates. The data depict the mean and standard deviation. pV = empty vector control.
(TIF)

S7 Fig. *hcp4* transcript is the most abundant within the operon. RNA coverage of all T6SS4 genes from samples of YPIII wt, incubated for 2 h at 25°C. Data was taken from Meyer *et al*., 2024 [46].
(TIF)

Acknowledgments

We would like to thank Dr. Ann-Kathrin Heroven for constructing the *lon* deletion mutant. We also thank the members of the Institute of Infectiology for helpful discussions throughout the course of this project.

Financial disclosure statement

This work was supported by the University of Münster (AK, BK, IM, YT, CSK, IPS, PD, ASH) and the German Research Foundation (DFG), with grant No. DFG-STO1208/2–1 given to ASH, and grant of the priority programme SPP2002 grant No. DFG DE616/7–2 given to P. Dersch.

The funders had no role in study design, data collection and analysis, decision to publish, or preparation of the manuscript.

Author contributions

Conceptualization: Anna Kerwien, Petra Dersch, Anne-Sophie Herbrüggen.

Data curation: Anna Kerwien.

Formal analysis: Anna Kerwien.

Funding acquisition: Petra Dersch, Anne-Sophie Herbrüggen.

Investigation: Anna Kerwien, Britta Körner, Ines Meyer, Yannick Teschke, Ileana Paula Salto, Anne-Sophie Herbrüggen.

Methodology: Anna Kerwien, Anne-Sophie Herbrüggen.

Project administration: Petra Dersch, Anne-Sophie Herbrüggen.

Resources: Cassandra Sophie Köster.

Supervision: Petra Dersch, Anne-Sophie Herbrüggen.

Validation: Anna Kerwien, Britta Körner, Ines Meyer, Yannick Teschke, Petra Dersch, Anne-Sophie Herbrüggen.

Visualization: Anna Kerwien.

Writing – original draft: Anna Kerwien, Petra Dersch.

Writing – review & editing: Britta Körner, Ines Meyer, Yannick Teschke, Cassandra Sophie Köster, Ileana Paula Salto, Anne-Sophie Herbrüggen.

References

1. Carniel E, Autenrieth I, Cornelis G, Fukushima H, Guinet F, Isberg R, et al. *Y. enterocolitica* and *Y. pseudotuberculosis*. In: Dworkin M, Falkow S, Rosenberg E, Schleifer K-H, Stackebrandt E, editors. The Prokaryotes: A Handbook on the Biology of Bacteria Volume 6: Proteobacteria: Gamma Subclass. New York (NY): Springer; 2006, p. 270–398.
2. Fredriksson-Ahomaa M. Isolation of enteropathogenic Yersinia from non-human sources. Adv Exp Med Biol. 2012;954:97–105. https://doi.org/10.1007/978-1-4614-3561-7_12 PMID: 22782751
3. Fredriksson-Ahomaa M, Stolle A, Korkeala H. Molecular epidemiology of Yersinia enterocolitica infections. FEMS Immunol Med Microbiol. 2006;47(3):315–29. https://doi.org/10.1111/j.1574-695X.2006.00095.x PMID: 16872368
4. Koornhof HJ, Smego RA Jr, Nicol M. Yersiniosis. II: The pathogenesis of Yersinia infections. Eur J Clin Microbiol Infect Dis. 1999;18(2):87–112. https://doi.org/10.1007/s100960050237 PMID: 10219574
5. Righetti F, Nuss AM, Twittenhoff C, Beele S, Urban K, Will S, et al. Temperature-responsive in vitro RNA structurome of Yersinia pseudotuberculosis. Proc Natl Acad Sci U S A. 2016;113(26):7237–42. https://doi.org/10.1073/pnas.1523004113 PMID: 27298343

6. Nuss AM, Heroven AK, Waldmann B, Reinkensmeier J, Jarek M, Beckstette M, et al. Transcriptomic profiling of Yersinia pseudotuberculosis reveals reprogramming of the Crp regulon by temperature and uncovers Crp as a master regulator of small RNAs. PLoS Genet. 2015;11(3):e1005087. https://doi.org/10.1371/journal.pgen.1005087 PMID: 25816203
7. Bölin I, Portnoy DA, Wolf-Watz H. Expression of the temperature-inducible outer membrane proteins of yersiniae. Infect Immun. 1985;48(1):234–40. https://doi.org/10.1128/iai.48.1.234-240.1985 PMID: 3980086
8. Cornelis GR, Boland A, Boyd AP, Geuijen C, Iriarte M, Neyt C, et al. The virulence plasmid of Yersinia, an antihost genome. Microbiol Mol Biol Rev. 1998;62(4):1315–52. https://doi.org/10.1128/MMBR.62.4.1315-1352.1998 PMID: 9841674
9. Deng W, Marshall NC, Rowland JL, McCoy JM, Worrall LJ, Santos AS, et al. Assembly, structure, function and regulation of type III secretion systems. Nat Rev Microbiol. 2017;15(6):323–37. https://doi.org/10.1038/nrmicro.2017.20 PMID: 28392566
10. Sansonetti PJ. War and peace at mucosal surfaces. Nat Rev Immunol. 2004;4(12):953–64. https://doi.org/10.1038/nri1499 PMID: 15573130
11. Abby SS, Rocha EPC. The non-flagellar type III secretion system evolved from the bacterial flagellum and diversified into host-cell adapted systems. PLoS Genet. 2012;8(9):e1002983. https://doi.org/10.1371/journal.pgen.1002983 PMID: 23028376
12. Böhme K, Steinmann R, Kortmann J, Seekircher S, Heroven AK, Berger E, et al. Concerted actions of a thermo-labile regulator and a unique intergenic RNA thermosensor control Yersinia virulence. PLoS Pathog. 2012;8(2):e1002518. https://doi.org/10.1371/journal.ppat.1002518 PMID: 22359501
13. Hoe NP, Goguen JD. Temperature sensing in Yersinia pestis: translation of the LcrF activator protein is thermally regulated. J Bacteriol. 1993;175(24):7901–9. https://doi.org/10.1128/jb.175.24.7901-7909.1993 PMID: 7504666
14. Jackson MW, Silva-Herzog E, Plano GV. The ATP-dependent ClpXP and Lon proteases regulate expression of the Yersinia pestis type III secretion system via regulated proteolysis of YmoA, a small histone-like protein. Mol Microbiol. 2004;54(5):1364–78. https://doi.org/10.1111/j.1365-2958.2004.04353.x PMID: 15554975
15. Balderas D, Ohanyan M, Alvarez PA, Mettert E, Tanner N, Kiley PJ, et al. Repression by the H-NS/YmoA histone-like protein complex enables IscR dependent regulation of the Yersinia T3SS. PLoS Genet. 2022;18(7):e1010321. https://doi.org/10.1371/journal.pgen.1010321 PMID: 35901167
16. Böhme K, Heroven AK, Lobedann S, Guo Y, Stolle A-S, Dersch P. The Small Protein YmoA Controls the Csr System and Adjusts Expression of Virulence-Relevant Traits of Yersinia pseudotuberculosis. Front Microbiol. 2021;12:706934. https://doi.org/10.3389/fmicb.2021.706934 PMID: 34413840
17. Cornelis GR, Sluiters C, Delor I, Geib D, Kaniga K, Lambert de Rouvroit C, et al. ymoA, a Yersinia enterocolitica chromosomal gene modulating the expression of virulence functions. Mol Microbiol. 1991;5(5):1023–34. https://doi.org/10.1111/j.1365-2958.1991.tb01875.x PMID: 1956283
18. Zhang W, Xu S, Li J, Shen X, Wang Y, Yuan Z. Modulation of a thermoregulated type VI secretion system by AHL-dependent quorum sensing in Yersinia pseudotuberculosis. Arch Microbiol. 2011;193(5):351–63. https://doi.org/10.1007/s00203-011-0680-2 PMID: 21298257
19. Pukatzki S, Ma AT, Sturtevant D, Krastins B, Sarracino D, Nelson WC, et al. Identification of a conserved bacterial protein secretion system in Vibrio cholerae using the Dictyostelium host model system. Proc Natl Acad Sci U S A. 2006;103(5):1528–33. https://doi.org/10.1073/pnas.0510322103 PMID: 16432199
20. Boyer F, Fichant G, Berthod J, Vandenbrouck Y, Attree I. Dissecting the bacterial type VI secretion system by a genome wide in silico analysis: what can be learned from available microbial genomic resources?. BMC Genomics. 2009;10:104. https://doi.org/10.1186/1471-2164-10-104 PMID: 19284603
21. Mougous JD, Cuff ME, Raunser S, Shen A, Zhou M, Gifford CA, et al. A virulence locus of Pseudomonas aeruginosa encodes a protein secretion apparatus. Science. 2006;312(5779):1526–30. https://doi.org/10.1126/science.1128393 PMID: 16763151
22. Basler M, Ho BT, Mekalanos JJ. Tit-for-tat: type VI secretion system counterattack during bacterial cell-cell interactions. Cell. 2013;152(4):884–94. https://doi.org/10.1016/j.cell.2013.01.042 PMID: 23415234
23. Sana TG, Baumann C, Merdes A, Soscia C, Rattei T, Hachani A, et al. Internalization of Pseudomonas aeruginosa Strain PAO1 into Epithelial Cells Is Promoted by Interaction of a T6SS Effector with the Microtubule Network. mBio. 2015;6(3):e00712. https://doi.org/10.1128/mBio.00712-15 PMID: 26037124
24. Fridman CM, Keppel K, Gerlic M, Bosis E, Salomon D. A comparative genomics methodology reveals a widespread family of membrane-disrupting T6SS effectors. Nat Commun. 2020;11(1):1085. https://doi.org/10.1038/s41467-020-14951-4 PMID: 32109231
25. Russell AB, Hood RD, Bui NK, LeRoux M, Vollmer W, Mougous JD. Type VI secretion delivers bacteriolytic effectors to target cells. Nature. 2011;475(7356):343–7. https://doi.org/10.1038/nature10244 PMID: 21776080
26. Basler M, Pilhofer M, Henderson GP, Jensen GJ, Mekalanos JJ. Type VI secretion requires a dynamic contractile phage tail-like structure. Nature. 2012;483(7388):182–6. https://doi.org/10.1038/nature10846 PMID: 22367545
27. Kenniston JA, Baker TA, Fernandez JM, Sauer RT. Linkage between ATP consumption and mechanical unfolding during the protein processing reactions of an AAA+ degradation machine. Cell. 2003;114(4):511–20. https://doi.org/10.1016/s0092-8674(03)00612-3 PMID: 12941278
28. Schlieker C, Zentgraf H, Dersch P, Mogk A. ClpV, a unique Hsp100/Clp member of pathogenic proteobacteria. Biol Chem. 2005;386(11):1115–27. https://doi.org/10.1515/BC.2005.128 PMID: 16307477
29. Bönemann G, Pietrosiuk A, Diemand A, Zentgraf H, Mogk A. Remodelling of VipA/VipB tubules by ClpV-mediated threading is crucial for type VI protein secretion. EMBO J. 2009;28(4):315–25. https://doi.org/10.1038/emboj.2008.269 PMID: 19131969

30. Knittel V, Sadana P, Seekircher S, Stolle A-S, Körner B, Volk M, et al. RovC - a novel type of hexameric transcriptional activator promoting type VI secretion gene expression. PLoS Pathog. 2020;16(9):e1008552. https://doi.org/10.1371/journal.ppat.1008552 PMID: 32966346
31. Gueguen E, Durand E, Zhang XY, d'Amalric Q, Journet L, Cascales E. Expression of a Yersinia pseudotuberculosis Type VI Secretion System Is Responsive to Envelope Stresses through the OmpR Transcriptional Activator. PLoS One. 2013;8(6):e66615. https://doi.org/10.1371/journal.pone.0066615 PMID: 23840509
32. Guan J, Xiao X, Xu S, Gao F, Wang J, Wang T, et al. Roles of RpoS in Yersinia pseudotuberculosis stress survival, motility, biofilm formation and type VI secretion system expression. J Microbiol. 2015;53(9):633–42. https://doi.org/10.1007/s12275-015-0099-6 PMID: 26310305
33. Song Y, Xiao X, Li C, Wang T, Zhao R, Zhang W, et al. The dual transcriptional regulator RovM regulates the expression of AR3- and T6SS4-dependent acid survival systems in response to nutritional status in Yersinia pseudotuberculosis. Environ Microbiol. 2015;17(11):4631–45. https://doi.org/10.1111/1462-2920.12996 PMID: 26234561
34. Zhang W, Wang Y, Song Y, Wang T, Xu S, Peng Z, et al. A type VI secretion system regulated by OmpR in Yersinia pseudotuberculosis functions to maintain intracellular pH homeostasis. Environ Microbiol. 2013;15(2):557–69. https://doi.org/10.1111/1462-2920.12005 PMID: 23094603
35. Gebhardt MJ, Kambara TK, Ramsey KM, Dove SL. Widespread targeting of nascent transcripts by RsmA in Pseudomonas aeruginosa. Proc Natl Acad Sci U S A. 2020;117(19):10520–9. https://doi.org/10.1073/pnas.1917587117 PMID: 32332166
36. Heroven AK, Böhme K, Rohde M, Dersch P. A Csr-type regulatory system, including small non-coding RNAs, regulates the global virulence regulator RovA of Yersinia pseudotuberculosis through RovM. Mol Microbiol. 2008;68(5):1179–95. https://doi.org/10.1111/j.1365-2958.2008.06218.x PMID: 18430141
37. Gore AL, Payne SM. CsrA and Cra influence Shigella flexneri pathogenesis. Infect Immun. 2010;78(11):4674–82. https://doi.org/10.1128/IAI.00589-10 PMID: 20713625
38. Butz HA, Mey AR, Ciosek AL, Crofts AA, Davies BW, Payne SM. Regulatory effects of CsrA in Vibrio cholerae. 2021;12.
39. Allsopp LP, Wood TE, Howard SA, Maggiorelli F, Nolan LM, Wettstadt S, et al. RsmA and AmrZ orchestrate the assembly of all three type VI secretion systems in Pseudomonas aeruginosa. Proc Natl Acad Sci U S A. 2017;114(29):7707–12. https://doi.org/10.1073/pnas.1700286114 PMID: 28673999
40. Wang T, Si M, Song Y, Zhu W, Gao F, Wang Y, et al. Type VI Secretion System Transports Zn2+ to Combat Multiple Stresses and Host Immunity. PLoS Pathog. 2015;11(7):e1005020. https://doi.org/10.1371/journal.ppat.1005020 PMID: 26134274
41. Cai R, Gao F, Pan J, Hao X, Yu Z, Qu Y, et al. The transcriptional regulator Zur regulates the expression of ZnuABC and T6SS4 in response to stresses in Yersinia pseudotuberculosis. Microbiol Res. 2021;249:126787. https://doi.org/10.1016/j.micres.2021.126787 PMID: 33991717
42. Zuo Y, Li C, Yu D, Wang K, Liu Y, Wei Z, et al. A Fur-regulated type VI secretion system contributes to oxidative stress resistance and virulence in Yersinia pseudotuberculosis. Stress Biol. 2023;3(1):2. https://doi.org/10.1007/s44154-022-00081-y PMID: 37676351
43. Zhu L, Xu L, Wang C, Li C, Li M, Liu Q, et al. T6SS translocates a micropeptide to suppress STING-mediated innate immunity by sequestering manganese. Proc Natl Acad Sci U S A. 2021;118(42):e2103526118. https://doi.org/10.1073/pnas.2103526118 PMID: 34625471
44. Avican K, Fahlgren A, Huss M, Heroven AK, Beckstette M, Dersch P, et al. Reprogramming of Yersinia from virulent to persistent mode revealed by complex in vivo RNA-seq analysis. PLoS Pathog. 2015;11(1):e1004600. https://doi.org/10.1371/journal.ppat.1004600 PMID: 25590628
45. Nuss AM, Beckstette M, Pimenova M, Schmühl C, Opitz W, Pisano F, et al. Tissue dual RNA-seq allows fast discovery of infection-specific functions and riboregulators shaping host-pathogen transcriptomes. Proc Natl Acad Sci U S A. 2017;114(5):E791–800. https://doi.org/10.1073/pnas.1613405114 PMID: 28096329
46. Meyer I, Volk M, Salto I, Moesser T, Chaoprasid P, Herbrüggen A-S, et al. RNase-mediated reprogramming of Yersinia virulence. PLoS Pathog. 2024;20(8):e1011965. https://doi.org/10.1371/journal.ppat.1011965 PMID: 39159284
47. Avican K, Aldahdooh J, Togninalli M, Mahmud AKMF, Tang J, Borgwardt KM, et al. RNA atlas of human bacterial pathogens uncovers stress dynamics linked to infection. Nat Commun. 2021;12(1):3282. https://doi.org/10.1038/s41467-021-23588-w PMID: 34078900
48. Stolle A-S, Meader BT, Toska J, Mekalanos JJ. Endogenous membrane stress induces T6SS activity in Pseudomonas aeruginosa. Proc Natl Acad Sci U S A. 2021;118(1):e2018365118. https://doi.org/10.1073/pnas.2018365118 PMID: 33443205
49. Basler M, Mekalanos JJ. Type 6 secretion dynamics within and between bacterial cells. Science. 2012;337(6096):815. https://doi.org/10.1126/science.1222901 PMID: 22767897
50. Jana B, Keppel K, Fridman CM, Bosis E, Salomon D. Multiple T6SSs, Mobile Auxiliary Modules, and Effectors Revealed in a Systematic Analysis of the Vibrio parahaemolyticus Pan-Genome. mSystems. 2022;7(6):e0072322. https://doi.org/10.1128/msystems.00723-22 PMID: 36226968
51. Lin L, Ringel PD, Vettiger A, Dürr L, Basler M. DNA Uptake upon T6SS-Dependent Prey Cell Lysis Induces SOS Response and Reduces Fitness of Acinetobacter baylyi. Cell Rep. 2019;29(6):1633-1644.e4. https://doi.org/10.1016/j.celrep.2019.09.083 PMID: 31693901
52. Brunet YR, Espinosa L, Harchouni S, Mignot T, Cascales E. Imaging type VI secretion-mediated bacterial killing. Cell Rep. 2013;3(1):36–41. https://doi.org/10.1016/j.celrep.2012.11.027 PMID: 23291094
53. George M, Narayanan S, Tejada-Arranz A, Plack A, Basler M. Initiation of H1-T6SS dueling between Pseudomonas aeruginosa. mBio. 2024;15(8):e0035524. https://doi.org/10.1128/mbio.00355-24 PMID: 38990002
54. Bissonnette SA, Rivera-Rivera I, Sauer RT, Baker TA. The IbpA and IbpB small heat-shock proteins are substrates of the AAA+ Lon protease. Mol Microbiol. 2010;75(6):1539–49. https://doi.org/10.1111/j.1365-2958.2010.07070.x PMID: 20158612

55. García-Fruitós E, Martínez-Alonso M, Gonzàlez-Montalbán N, Valli M, Mattanovich D, Villaverde A. Divergent genetic control of protein solubility and conformational quality in Escherichia coli. J Mol Biol. 2007;374(1):195–205. https://doi.org/10.1016/j.jmb.2007.09.004 PMID: 17920630

56. Laskowska E, Kuczyńska-Wiśnik D, Skórko-Glonek J, Taylor A. Degradation by proteases Lon, Clp and HtrA, of Escherichia coli proteins aggregated in vivo by heat shock; HtrA protease action in vivo and in vitro. Mol Microbiol. 1996;22(3):555–71. https://doi.org/10.1046/j.1365-2958.1996.1231493.x PMID: 8939438

57. Sakr S, Cirinesi A-M, Ullers RS, Schwager F, Georgopoulos C, Genevaux P. Lon protease quality control of presecretory proteins in Escherichia coli and its dependence on the SecB and DnaJ (Hsp40) chaperones. J Biol Chem. 2010;285(30):23506–14. https://doi.org/10.1074/jbc.M110.133058 PMID: 20504766

58. Schoemaker JM, Gayda RC, Markovitz A. Regulation of cell division in Escherichia coli: SOS induction and cellular location of the sulA protein, a key to lon-associated filamentation and death. J Bacteriol. 1984;158(2):551–61. https://doi.org/10.1128/jb.158.2.551-561.1984 PMID: 6327610

59. Torres-Cabassa AS, Gottesman S. Capsule synthesis in Escherichia coli K-12 is regulated by proteolysis. J Bacteriol. 1987;169(3):981–9. https://doi.org/10.1128/jb.169.3.981-989.1987 PMID: 3029041

60. Jackson MW, Silva-Herzog E, Plano GV. The ATP-dependent ClpXP and Lon proteases regulate expression of the Yersinia pestis type III secretion system via regulated proteolysis of YmoA, a small histone-like protein. Mol Microbiol. 2004;54(5):1364–78. https://doi.org/10.1111/j.1365-2958.2004.04353.x PMID: 15554975

61. Herbst K, Bujara M, Heroven AK, Opitz W, Weichert M, Zimmermann A, et al. Intrinsic thermal sensing controls proteolysis of Yersinia virulence regulator RovA. PLoS Pathog. 2009;5(5):e1000435. https://doi.org/10.1371/journal.ppat.1000435 PMID: 19468295

62. Förstner KU, Reuscher CM, Haberzettl K, Weber L, Klug G. RNase E cleavage shapes the transcriptome of *Rhodobacter sphaeroides* and strongly impacts phototrophic growth. Life Sci Alliance. 2018;1(4):e201800080. https://doi.org/10.26508/lsa.201800080 PMID: 30456366

63. Spanka D-T, Reuscher CM, Klug G. Impact of PNPase on the transcriptome of Rhodobacter sphaeroides and its cooperation with RNase III and RNase E. BMC Genomics. 2021;22(1):106. https://doi.org/10.1186/s12864-021-07409-4 PMID: 33549057

64. Broglia L, Materne S, Lécrivain A-L, Hahnke K, Le Rhun A, Charpentier E. RNase Y-mediated regulation of the streptococcal pyrogenic exotoxin B. RNA Biol. 2018;15(10):1336–47. https://doi.org/10.1080/15476286.2018.1532253 PMID: 30290721

65. Zuker M. Mfold web server for nucleic acid folding and hybridization prediction. Nucleic Acids Res. 2003;31(13):3406–15. https://doi.org/10.1093/nar/gkg595 PMID: 12824337

66. Armbruster CR, Lee CK, Parker-Gilham J, de Anda J, Xia A, Zhao K, et al. Heterogeneity in surface sensing suggests a division of labor in Pseudomonas aeruginosa populations. Elife. 2019;8:e45084. https://doi.org/10.7554/eLife.45084 PMID: 31180327

67. Dubnau D, Losick R. Bistability in bacteria. Mol Microbiol. 2006;61(3):564–72. https://doi.org/10.1111/j.1365-2958.2006.05249.x PMID: 16879639

68. Ackermann M. A functional perspective on phenotypic heterogeneity in microorganisms. Nat Rev Microbiol. 2015;13(8):497–508. https://doi.org/10.1038/nrmicro3491 PMID: 26145732

69. Balaban NQ, Merrin J, Chait R, Kowalik L, Leibler S. Bacterial persistence as a phenotypic switch. Science. 2004;305(5690):1622–5. https://doi.org/10.1126/science.1099390 PMID: 15308767

70. Ratcliff WC, Denison RF. Individual-level bet hedging in the bacterium Sinorhizobium meliloti. Curr Biol. 2010;20(19):1740–4. https://doi.org/10.1016/j.cub.2010.08.036 PMID: 20869244

71. Solopova A, van Gestel J, Weissing FJ, Bachmann H, Teusink B, Kok J, et al. Bet-hedging during bacterial diauxic shift. Proc Natl Acad Sci U S A. 2014;111(20):7427–32. https://doi.org/10.1073/pnas.1320063111 PMID: 24799698

72. Weigel WA, Dersch P. Phenotypic heterogeneity: a bacterial virulence strategy. Microbes Infect. 2018;20(9–10):570–7. https://doi.org/10.1016/j.micinf.2018.01.008 PMID: 29409898

73. Herbst K, Bujara M, Heroven AK, Opitz W, Weichert M, Zimmermann A, et al. Intrinsic thermal sensing controls proteolysis of Yersinia virulence regulator RovA. PLoS Pathog. 2009;5(5):e1000435. https://doi.org/10.1371/journal.ppat.1000435 PMID: 19468295

74. Nagel G, Lahrz A, Dersch P. Environmental control of invasin expression in Yersinia pseudotuberculosis is mediated by regulation of RovA, a transcriptional activator of the SlyA/Hor family. Mol Microbiol. 2001;41(6):1249–69. https://doi.org/10.1046/j.1365-2958.2001.02522.x PMID: 11580832

75. Nuss AM, Schuster F, Roselius L, Klein J, Bücker R, Herbst K, et al. A Precise Temperature-Responsive Bistable Switch Controlling Yersinia Virulence. PLoS Pathog. 2016;12(12):e1006091. https://doi.org/10.1371/journal.ppat.1006091 PMID: 28006011

76. Taillefer B, Schattenberg F, Doan T, Müller S, Cascales E. BioRxiv [Preprint] Type VI secretion phenotypic heterogeneity ensures trade-off between antibacterial activity and resistance in Enteroaggregative *E. coli*. 2025. https://doi.org/10.1101/2025.02.11.637775

77. Dar D, Sorek R. Extensive reshaping of bacterial operons by programmed mRNA decay. PLoS Genet. 2018;14(4):e1007354. https://doi.org/10.1371/journal.pgen.1007354 PMID: 29668692

78. Richards J, Belasco JG. Obstacles to Scanning by RNase E Govern Bacterial mRNA Lifetimes by Hindering Access to Distal Cleavage Sites. Mol Cell. 2019;74(2):284-295.e5. https://doi.org/10.1016/j.molcel.2019.01.044 PMID: 30852060

79. Arnold TE, Yu J, Belasco JG. mRNA stabilization by the ompA 5' untranslated region: two protective elements hinder distinct pathways for mRNA degradation. RNA. 1998;:319–30.

80. Komarova AV, Tchufistova LS, Dreyfus M, Boni IV. AU-rich sequences within 5' untranslated leaders enhance translation and stabilize mRNA in Escherichia coli. J Bacteriol. 2005;187(4):1344–9. https://doi.org/10.1128/JB.187.4.1344-1349.2005 PMID: 15687198

81. Emory SA, Bouvet P, Belasco JG. A 5'-terminal stem-loop structure can stabilize mRNA in Escherichia coli. Genes Dev. 1992;6(1):135–48. https://doi.org/10.1101/gad.6.1.135 PMID: 1370426
82. Chen F, Cocaign-Bousquet M, Girbal L, Nouaille S. 5'UTR sequences influence protein levels in Escherichia coli by regulating translation initiation and mRNA stability. Front Microbiol. 2022;13:1088941. https://doi.org/10.3389/fmicb.2022.1088941 PMID: 36620028
83. Adams PP, Baniulyte G, Esnault C, Chegireddy K, Singh N, Monge M, et al. Regulatory roles of Escherichia coli 5' UTR and ORF-internal RNAs detected by 3' end mapping. Elife. 2021;10:e62438. https://doi.org/10.7554/eLife.62438 PMID: 33460557
84. Caron M-P, Bastet L, Lussier A, Simoneau-Roy M, Massé E, Lafontaine DA. Dual-acting riboswitch control of translation initiation and mRNA decay. Proc Natl Acad Sci U S A. 2012;109(50):E3444-53. https://doi.org/10.1073/pnas.1214024109 PMID: 23169642
85. Amilon KR, Letley DP, Winter JA, Robinson K, Atherton JC. Expression of the Helicobacter pylori virulence factor vacuolating cytotoxin A (vacA) is influenced by a potential stem-loop structure in the 5' untranslated region of the transcript. Mol Microbiol. 2015;98(5):831–46. https://doi.org/10.1111/mmi.13160 PMID: 26259667
86. Lin L, Lezan E, Schmidt A, Basler M. Abundance of bacterial Type VI secretion system components measured by targeted proteomics. Nat Commun. 2019;10(1):2584. https://doi.org/10.1038/s41467-019-10466-9 PMID: 31197144
87. Li G-W, Burkhardt D, Gross C, Weissman JS. Quantifying absolute protein synthesis rates reveals principles underlying allocation of cellular resources. Cell. 2014;157(3):624–35. https://doi.org/10.1016/j.cell.2014.02.033 PMID: 24766808
88. Quax TEF, Wolf YI, Koehorst JJ, Wurtzel O, van der Oost R, Ran W, et al. Differential translation tunes uneven production of operon-encoded proteins. Cell Rep. 2013;4(5):938–44. https://doi.org/10.1016/j.celrep.2013.07.049 PMID: 24012761
89. Newbury SF, Smith NH, Higgins CF. Differential mRNA stability controls relative gene expression within a polycistronic operon. Cell. 1987;51(6):1131–43. https://doi.org/10.1016/0092-8674(87)90599-x PMID: 2446776
90. Desnoyers G, Morissette A, Prévost K, Massé E. Small RNA-induced differential degradation of the polycistronic mRNA iscRSUA. EMBO J. 2009;28(11):1551–61. https://doi.org/10.1038/emboj.2009.116 PMID: 19407815
91. Nilsson P, Uhlin BE. Differential decay of a polycistronic Escherichia coli transcript is initiated by RNaseE-dependent endonucleolytic processing. Mol Microbiol. 1991;5(7):1791–9. https://doi.org/10.1111/j.1365-2958.1991.tb01928.x PMID: 1943710
92. Naureckiene S, Uhlin BE. In vitro analysis of mRNA processing by RNase E in the pap operon of Escherichia coli. Mol Microbiol. 1996;21(1):55–68. https://doi.org/10.1046/j.1365-2958.1996.6121101.x PMID: 8843434
93. Heck C, Balzer A, Fuhrmann O, Klug G. Initial events in the degradation of the polycistronic puf mRNA in Rhodobacter capsulatus and consequences for further processing steps. Mol Microbiol. 2000;35(1):90–100. https://doi.org/10.1046/j.1365-2958.2000.01679.x PMID: 10632880
94. Chen CY, Beatty JT, Cohen SN, Belasco JG. An intercistronic stem-loop structure functions as an mRNA decay terminator necessary but insufficient for *puf* mRNA stability. Cell. 1988;52(4):609–19. https://doi.org/10.1016/0092-8674(88)90473-4 PMID: 2449287
95. Bricker AL, Belasco JG. Importance of a 5' stem-loop for longevity of papA mRNA in Escherichia coli. J Bacteriol. 1999;181(11):3587–90. https://doi.org/10.1128/JB.181.11.3587-3590.1999 PMID: 10348874
96. Zhai W, Duan Y, Zhang X, Xu G, Li H, Shi J, et al. Sequence and thermodynamic characteristics of terminators revealed by FlowSeq and the discrimination of terminators strength. Synth Syst Biotechnol. 2022;7(4):1046–55. https://doi.org/10.1016/j.synbio.2022.06.003 PMID: 35845313
97. McLaren RS, Newburyl SF, Dance GSC, Causton HC, Higgins CF. mRNA Degradation by Processive 3'4' Exoribonucleases in vitro and the Implications for Prokaryotic mRNA Decay. J Mol Biol. 1991;:81–95.
98. Durand E, Nguyen VS, Zoued A, Logger L, Péhau-Arnaudet G, Aschtgen M-S, et al. Biogenesis and structure of a type VI secretion membrane core complex. Nature. 2015;523(7562):555–60. https://doi.org/10.1038/nature14667 PMID: 26200339
99. Basler M. Type VI secretion system: secretion by a contractile nanomachine. Philos Trans R Soc Lond B Biol Sci. 2015;370(1679):20150021. https://doi.org/10.1098/rstb.2015.0021 PMID: 26370934
100. Wang J, Brackmann M, Castaño-Díez D, Kudryashev M, Goldie KN, Maier T, et al. Cryo-EM structure of the extended type VI secretion system sheath-tube complex. Nat Microbiol. 2017;2(11):1507–12. https://doi.org/10.1038/s41564-017-0020-7 PMID: 28947741
101. Mougous JD, Gifford CA, Ramsdell TL, Mekalanos JJ. Threonine phosphorylation post-translationally regulates protein secretion in Pseudomonas aeruginosa. Nat Cell Biol. 2007;9(7):797–803. https://doi.org/10.1038/ncb1605 PMID: 17558395
102. Pietrosiuk A, Lenherr ED, Falk S, Bönemann G, Kopp J, Zentgraf H, et al. Molecular basis for the unique role of the AAA+ chaperone ClpV in type VI protein secretion. J Biol Chem. 2011;286(34):30010–21. https://doi.org/10.1074/jbc.M111.253377 PMID: 21733841
103. Wu H-Y, Chung P-C, Shih H-W, Wen S-R, Lai E-M. Secretome analysis uncovers an Hcp-family protein secreted via a type VI secretion system in Agrobacterium tumefaciens. J Bacteriol. 2008;190(8):2841–50. https://doi.org/10.1128/JB.01775-07 PMID: 18263727
104. Zhou Y, Tao J, Yu H, Ni J, Zeng L, Teng Q, et al. Hcp family proteins secreted via the type VI secretion system coordinately regulate Escherichia coli K1 interaction with human brain microvascular endothelial cells. Infect Immun. 2012;80(3):1243–51. https://doi.org/10.1128/IAI.05994-11 PMID: 22184413
105. Zheng J, Ho B, Mekalanos JJ. Genetic analysis of anti-amoebae and anti-bacterial activities of the type VI secretion system in Vibrio cholerae. PLoS One. 2011;6(8):e23876. https://doi.org/10.1371/journal.pone.0023876 PMID: 21909372
106. Zhang A, Han Y, Huang Y, Hu X, Liu P, Liu X, et al. vgrG is separately transcribed from hcp in T6SS orphan clusters and is under the regulation of IHF and HapR. Biochem Biophys Res Commun. 2021;559:15–20. https://doi.org/10.1016/j.bbrc.2021.04.092 PMID: 33932896

107. Rojas AM, Rios JEG de L, Saux MF-L, Jimenez P, Reche P, Bonneau S, et al. Erwinia toletana sp. nov., associated with Pseudomonas savastanoi-induced tree knots. Int J Syst Evol Microbiol. 2004;54(Pt 6):2217–22. https://doi.org/10.1099/ijs.0.02924-0 PMID: 15545461

108. Hosni T, Moretti C, Devescovi G, Suarez-Moreno ZR, Fatmi MB, Guarnaccia C, et al. Sharing of quorum-sensing signals and role of interspecies communities in a bacterial plant disease. ISME J. 2011;5(12):1857–70. https://doi.org/10.1038/ismej.2011.65 PMID: 21677694

109. Brady C, Kaur S, Crampton B, Maddock D, Arnold D, Denman S. Transfer of Erwinia toletana and Erwinia iniecta to a novel genus Winslowiella gen. nov. as Winslowiella toletana comb. nov. and Winslowiella iniecta comb. nov. and description of Winslowiella arboricola sp. nov., isolated from bleeding cankers on broadleaf hosts. Front Microbiol. 2022;13:1063107. https://doi.org/10.3389/fmicb.2022.1063107 PMID: 36466697

110. Chou J-H, Chen W-M, Arun AB, Young C-C. Trabulsiella odontotermitis sp. nov., isolated from the gut of the termite Odontotermes formosanus Shiraki. Int J Syst Evol Microbiol. 2007;57(Pt 4):696–700. https://doi.org/10.1099/ijs.0.64632-0 PMID: 17392189

111. Sapountzis P, Gruntjes T, Otani S, Estevez J, da Costa RR, Plunkett G 3rd, et al. The Enterobacterium Trabulsiella odontotermitis Presents Novel Adaptations Related to Its Association with Fungus-Growing Termites. Appl Environ Microbiol. 2015;81(19):6577–88. https://doi.org/10.1128/AEM.01844-15 PMID: 26162887

112. McWhorter AC, Haddock RL, Nocon FA, Steigerwalt AG, Brenner DJ, Aleksić S, et al. Trabulsiella guamensis, a new genus and species of the family Enterobacteriaceae that resembles *Salmonella* subgroups 4 and 5. J Clin Microbiol. 1991;29(7):1480–5. https://doi.org/10.1128/jcm.29.7.1480-1485.1991 PMID: 1885744

113. Patil VS, Salunkhe RC, Patil RH, Husseneder C, Shouche YS, Venkata Ramana V. Enterobacillus tribolii gen. nov., sp. nov., a novel member of the family Enterobacteriaceae, isolated from the gut of a red flour beetle, *Tribolium castaneum*. Antonie Van Leeuwenhoek. 2015;107(5):1207–16. https://doi.org/10.1007/s10482-015-0412-8 PMID: 25716888

114. Aljorayid A, Viau R, Castellino L, Jump RLP. Serratia fonticola, pathogen or bystander? A case series and review of the literature. IDCases. 2016;5:6–8. https://doi.org/10.1016/j.idcr.2016.05.003 PMID: 27347484

115. Gavini F, Ferragut C, Izard D, Trinel Pa, Leclerc H, Lefebvre B, et al. Serratia fonticola, a New Species from Water. Int J Systemat Bacteriol. 1979;29(2):92–101. https://doi.org/10.1099/00207713-29-2-92

116. Scouten JM, Hsieh S-C, Sung L-K, Wen Y-HV, Kuo C-H, Lai E-M, et al. Function, Evolution, and Ecology of Type VI Secretion Systems of Plant-Associated Bacteria. Environmental Microbiology. 2025;20: 1–115. htpps://doi.org/10.1111/1462-2920.13956

117. Gilchrist CLM, Chooi Y-H. clinker & clustermap.js: automatic generation of gene cluster comparison figures. Bioinformatics. 2021;37(16):2473–5. https://doi.org/10.1093/bioinformatics/btab007 PMID: 33459763

118. Hanahan D. Studies on transformation of Escherichia coli with plasmids. J Mol Biol. 1983;166(4):557–80. https://doi.org/10.1016/s0022-2836(83)80284-8 PMID: 6345791

119. Gibson DG, Young L, Chuang R-Y, Venter JC, Hutchison CA 3rd, Smith HO. Enzymatic assembly of DNA molecules up to several hundred kilobases. Nat Methods. 2009;6(5):343–5. https://doi.org/10.1038/nmeth.1318 PMID: 19363495

120. Ho SN, Hunt HD, Horton RM, Pullen JK, Pease LR. Site-directed mutagenesis by overlap extension using the polymerase chain reaction. Gene. 1989;77(1):51–9. https://doi.org/10.1016/0378-1119(89)90358-2 PMID: 2744487

121. Heroven AK, Sest M, Pisano F, Scheb-Wetzel M, Steinmann R, Böhme K, et al. Crp induces switching of the CsrB and CsrC RNAs in Yersinia pseudotuberculosis and links nutritional status to virulence. Front Cell Infect Microbiol. 2012;2:158. https://doi.org/10.3389/fcimb.2012.00158 PMID: 23251905

122. Hmelo LR, Borlee BR, Almblad H, Love ME, Randall TE, Tseng BS, et al. Precision-engineering the Pseudomonas aeruginosa genome with two-step allelic exchange. Nat Protoc. 2015;10(11):1820–41. https://doi.org/10.1038/nprot.2015.115 PMID: 26492139

123. Datsenko KA, Wanner BL. One-step inactivation of chromosomal genes in Escherichia coli K-12 using PCR products. Proc Natl Acad Sci U S A. 2000;97(12):6640–5. https://doi.org/10.1073/pnas.120163297 PMID: 10829079

124. Cherepanov PP, Wackernagel W. Gene disruption in *Escherichia coli*: TcR and KmR cassettes with the option of Flp-catalyzed excision of the antibiotic-resistance determinant. Gene. 1995;158(1):9–14. https://doi.org/10.1016/0378-1119(95)00193-a PMID: 7789817

125. Livak KJ, Schmittgen TD. Analysis of relative gene expression data using real-time quantitative PCR and the 2(-Delta Delta C(T)) Method. Methods. 2001;25(4):402–8. https://doi.org/10.1006/meth.2001.1262 PMID: 11846609

126. Laemmli UK. Cleavage of structural proteins during the assembly of the head of bacteriophage T4. Nature. 1970;227(5259):680–5. https://doi.org/10.1038/227680a0 PMID: 5432063

127. Miller J. Experiments in molecular genetics. New York: Cold Spring Habor; 1972.